ANATOMICAL RELATIONSHIP BETWEEN THE BIOLOGICAL CLOCK AND THE NEUROENDOCRINE HYPOTHALAMUS

Dr. Tamás L. Horváth

Department of Obstetrics and Gynecology
Yale University School of Medicine

NEW HAVEN
1998

TABLE OF CONTENTS:

OBJECTIVES

The biological clock located in the hypothalamic suprachiasmatic nucleus (SCN) in conjunction with the intergeniculate leaflet of the lateral geniculate body (IGL) provide circadian and visual signals for the temporal organization of endocrine and autonomic mechanisms supporting higher brain functions. One component of clock-driven endocrine mechanisms is the circadian gonadotropin and lactotrop hormone secretions from the anterior pituitary that is pivotal for the maintenance of normal reproduction in all species thus far studied.

The pituitary secretion of gonadotrop hormones, luteinizing hormone releasing hormone (LH) and follice stimulating hormone (FSH), and the lactotrop hormone, prolactin are under the regulation of the hypothalamus. In the hypothalamus, humoral signals arising from the gonads (testosterone, estradiol and progesterone) and neuronal signals arising from the circadian clock are integrated to regulate the final output neurons of the hypothalamus underlying pituitary gonadotropin and prolactin secretions, the gonadortopin releasing hormone (GnRH)- and dopamine-producing neural circuits. The circadian activity of the rat hypothalamo-pituitary axis is gender specific, only females having the ability to manifest surges of gonadotropin and prolactin releases in response to elevating estradiol and progesterone levels and adequate circadian signals. While a large body of morphological and physiological evidence has accumulated to explain these gender specific endocrine mechanisms, the signaling pathway from the circadian clock to neuroendocrine cells is ill defined. It is also not known whether the gender specific nature of pituitary hormone secretions may be supported by sex differences in the circadian clock and whether the integration of hormonal signals into the hypothalamo-pituitary axis may occur outside of the hypothalamus in part of the extended biological clock. Experiments in this thesis were designed to fill these *hiata* and, thus, gain further insights into the central regulation of anterior pituitary hormone secretions. The following specific objectives were to be tested:

1) Does the circadian clock, SCN, provides direct signals for neuroendocrine cells, including those producing GnRH and dopamine?
2) Can the IGL in the lateral geniculate body provide signals to neuroendocrine cells independent of the SCN?

3) Can gonadal signals be integrated into the hypothalamo-pituitary axis outside of the hypothalamus, in the IGL?
4) Is the development of the biological clock under the control of gonadal steroids?
5) Is the SCN input to GnRH cells gender specific?

To accomplish these aims, the combination of anterograde, retrograde tracing, degeneration techniques, light and electron microscopic immunocytochemistry, biochemical assays and *in situ* hybridization histochemistry were used.

BACKGROUND AND SIGNIFICANCE

The capacity of the central nervous system to carry out higher brain functions, including learning, memory processing, and cognition in general, is highly dependent on adequately organized autonomic and endocrine mechanisms. The disruption of synchrony between autonomic and endocrine mechanisms can underlie the emergence of psychosomatic symptoms that can temporally impair certain brain functions. For example, discomforting central nervous system side effects of declining circulating gonadal steroid levels can, in turn, lead to the emergence of such symptoms. The change in the hormonal milieu may be due to physiological events (menstrual cycle, pregnancy, post partum, premenstrual and perimenopausal periods) or can be the consequence of gonadectomy prompted by different neoplastic events, including endometrial or prostate cancer. Characteristic side effects of these hormonal alterations include unpredictable mood swings, anxiety, depression, temporal and erratic disturbances in thermoregulation (hot flushes; night sweats), altered sleep patterns and gonadotropin secretion (1-19). One of the possible consequences of these discomforting side effects of gonadal failure is impaired ability of an individual to carry out complex tasks while the symptoms occur (20).

The biological clock provides synchronized rhythms for central nervous system mechanisms

In the central nervous system of mammals, including humans, the syncronization of the activity of different brain mechanisms with each other and with the environment is largely organized by the biological clock (21, 22). In most species thus far studied, the main circadian clock resides in the suprachiasmatic nucleus (SCN) of the hypothalamus and is primarly entrained by the light/dark cycle via direct retinal projections to its core region (22-25). The SCN via paracrine action (26) and neural projections (27,28) affects a variety of regions and related functions of the brain (21, 22). The SCN also receives processed visual input via a subdivision of the thalamic lateral geniculate nucleus (LGN), i.e., the intergeniculate leaflet (IGL) of the LGN (29, 30). It has been suggested that the geniculohypothalamic tract exerts feedback action on the SCN, modulating the entrainment of circadian rhythms to the light-dark cycle after phase-shifting (22). Throughout this thesis, I will refer to the SCN-IGL complex as the *extended biological clock*.

The SCN and the anterior pituitary

Ovulation in females, which in rats occurs regularly in every four day, rigidly coincides with the appearance of lordosis behavior that allows males to mount and fertilize females. The central regulation of ovulation and related hormones is mediated through the hypothalamo-pituitary axis of which activity is entrained by SCN (31). While the pivotal role of SCN efferents in these regulatory mechanisms is evident, less is known about the fine neural circuits via the suprachiasmatic signals reach the target neuronal elements.

Secretion of anterior pituitary hormones including gonadotrophins and prolactin, is regulated by various hypothalamic neurohormones. It is known that the median eminence conveys both humoral and neural signals from the brain to the pituitary. In the external layer of the median eminence, the terminals of hypophysiotropic hormone-producing neurons release their products into the fenestrated portal capillaries that provide the link between the hypothalamus and the anterior pituitary (32). Neuroendocrine cells are located in various hypothalamic sites, including the medial preoptic area, periventricular areas and the mediobasal hypothalamus, as well as in the medial septum and diagonal band of Broca.

Previous morphological studies failed to demonstrate suprachiasmatic efferents in the median eminence or organum vasculosum laminae terminalis (28) indicating that the circadian clock has no direct effect on pituitary hormone secretion, but acts indirectly, through regulating the activity of hypophysiotropic hormone-producing neurons. In support of this view, several hypothalamic areas which contain median eminence-projective neurons, such as the medial preoptic area, periventricular areas, and lateral arcuate nucleus, were found to be targets of considerable amount of SCN efferents (27,28). However, it is not known whether those neurons that send projections to portal vessels receive inputs from the SCN.

Several neurotransmitter and peptide-producing hypothalamic neuronal population was shown to release their product to the portal vessels of the median eminence. These include GnRH and dopamine that are the mayor hypothalamic regulatory signals in gonadotropin and prolactin secretions, respectively (33). Evidence has accumulated indicating that synthesis and/or release of GnRH and dopamine show diurnal patterns. Despite this experimental evidence, our understanding regarding the morphological basis of the circadian secretory function of hyophysiotropic hormones and regulatory peptides is limited.

Objective 1 will address this by revealing the synaptological interaction between SCN efferents and neuroendocrine cells that project to the median eminence and produce either dopamine or GnRH.

The possible mediatory role of the IGL in anterior pituitary hormone secretions

The appropriate alternation of light/dark cycles and the interaction between the *visual*, circadian and neuroendocrine systems are essential in the maintenance of rhythmic secretion of prolactin and luteinizing hormone (34-37). For example, exposure to constant light induces the emergence of impaired LH and prolactin secretions leading to the failure of ovarian cycles (38-46).

It was postulated that a tightly coupled relationship exists between the retino-recipient suprachiasmatic nucleus (SCN) and the principal regulatory cells in gonadotropin and prolactin secretion, the luteinizing hormone-releasing hormone (GnRH)- and dopamine-producing neurons because: 1) there is a lack of SCN efferents in the median eminence, the site where neurohormones are released into the portal capillaries and are transported to the anterior pituitary; and 2) the GnRH and dopamine cells are located in areas of the hypothalamus that are targeted by SCN efferents (27,28,47-49). These observations suggested a signaling pathway for circadian regulation of the hypothalamo-pituitary axis and this path from the SCN to neuroendocrine cells wil be assesed in the first objective of this thesis. However, the constant light-induced malfunctioning of the anterior pituitary cannot be easily understood by this signaling modality: during constant light, the circadian pacemaker free runs (50). However, the circadian daily and preovulatory gonadotropin and prolactin secretions are abolished (38,39,43,45,46). While arrhythmicity in SCN activity was also detected in animals kept in constant light which could cause impaired hormone secretions (51), it may be that during exposure to constant light, photic stimuli can continuously reach neuroendocrine cells via a pathway that does not involve the SCN.

A brain region that has the potential to mediate *non-circadian* visual information to the hypothalamus is the intergeniculate leaflet (IGL) of the lateral geniculate nucleus (LGN): it receives direct visual input (52), has not been shown to have intrinsic circadian activity, and, cells of the IGL innervate extrasuprachiasmatic areas of the hypothalamus (53-55). Objective 2 will explore the interconnection between LGN efferents and neurons of the hypothalamus,

including those producing dopamine that are neuroendocrine, i.e., they have direct access to fenestrated capillaries. These cells can release their products to the portal vessels in the median eminence that provides the humoral link between the hypothalamus and the anterior pituitary. This study also aims to determine whether intergeniculate neurons that give rise to hypothalamic projections are direct targets of retinal axons. Furthermore, Objective 3 will determine whether gonadal steroid signals may di ectly affect neurons of the IGL.

The sexually dimorphic, circadian gonadotropin and prolactin secretion of the rat

GnRH and prolactin are secreted in a circadian and gender specific manner (56) into the portal vasculature at the level of the median eminence. It is well established that in rodents, females possess a neurogenic mechanism that allows the activation of the hypothalamic neuronal systems by estradiol (positive gonadotropin feedback) and thereby induces the ovulatory surge of LH, FSH and prolactin. Destruction of the biological clock (SCN) blocks the preovulatory LH and prolactin surges and induces persistent estrus in intact female rats (37). The preovulatory LH and prolactin surges occur once every 4 to 5 days in intact animals, but treatment of ovariectomized (OVX) female rats with estrogen (E) results in a daily (circadian) proestrus-like surge of LH and prolactin (57). Complete lesions of the SCN eliminate these daily LH and prolactin surges (38,58). In males, hypothalamic neurons are under tonic inhibition by circulating gonadal steroids and the positive feedback action of estradiol to induce circadian LH and prolactin secretions is absent (59). While sexual differentiation of the reproductive hypothalamus have been extensively studies, it is not known whether the emergence in sexual dimorphic anterior pituitary regulations is supported by gender differences in the circadian input to the hypothalamo-pituitary axis.

Sexually dimorphic morphology of the rat SCN has been demonstrated for a number of parameters. For example, three-dimensional images of the SCN of males and females showed that the volume of the SCN is larger in males (60,61) and contains more nuclei (62). Morphological studies demonstrated that SCN efferents, which contain vasopressin (63) or VIP (64), develop in a gender specific manner, as well. Although neonatal alteration of the hormonal environment is capable of reversing these sexually dimorphic features of both the SCN (60) and several circadian rhythms (65), it is not known whether a sexually dimorphic development of the circadian clock may be necessary for the maintenance of positive gonadotropin feedback.

Several areas of the rat brain show gender differences. Of these, the most extensively studied is located in the medial preoptic nucleus of the hypothalamus. Gorski et al. (66,67) reported that the so-called sexual dimorphic nucleus (SDN) of the medial preoptic area, is significantly bigger in males than in females. They demonstrated that this difference is due to the prenatal and neonatal levels of locally formed estradiol from testosterone (68-70) that are significantly higher in males than in females (71). While they succeeded in reversing the size of this nucleus in females by perinatal administration of testosterone (masculinization; 68,69), administration of dihydrotestosterone to females did not induce masculinization (72), but estradiol had a masculinizing effect (68,69). These findings demonstrated that during early development of the central nervous system, testosterone converted to estradiol by the enzyme *aromatase regulates the maturation and sexual differentiation* of brain areas.

The key enzyme for brain sexual differentiation, aromatase, is present in distinct nuclei of the central nervous system (73,74). In the CNS, biochemical approaches revealed the highest aromatase activity to be present in limbic structures, including the amygdala, hippocampus, bed nucleus of the stria terminalis, lateral septum, and medial preoptic area of the hypothalamus (75). Corresponding to the notion that aromatase is related to sexual phenotype, all of these limbic and hypothalamic areas participate in the regulation of reproductive functions.

The synaptology and efferent projections of the IGL and SCN start to develop from embryonic day (E) 16 and 19, respectively (76). This coincides with the appearance of aromatase immunoreactivity in the hypothalamus. Parallel changes in androgen levels can be seen with aromatase enzyme activity throughout this perinatal period in both males and females (77). Plasma testosterone levels of males start to elevate at E 17 and peak between E18 and 19. After a transient decrease, blood testosterone concentrations increase after birth (71, 78-80). Females also show a slight elevation in prenatal blood androgen levels, but even their peak values do not reach the male baseline levels (71). Aromatase immunoreactivity in the SCN, IGL and optic tract increases from E 18 until post-embryonic day (P) 20 (81,82). The distribution pattern and density of these axons stay at the same level until P 20, followed by a decrease (81,82). During this

perinatal period (E 18-P21), the afferent and efferent connections of the SCN and IGL are established (83).

The aforementioned morphological and pharmacological data gave impetus to our hypothesis that sexual dimorphism in anterior pituitary hormone secretion may be supported by gender specific characteristics of the extended biological clock. Objectives 4 and 5 of this thesis will test this hypothesis.

Significance to human health

The appropriate entrainment of brain functions to the environment is normally achieved by the circadian clock in all species thus far studied, including humans. Altered activity of the biological clock in the absence of gonadal hormones may be a key trigger in initiating and maintaining the discomforting side effects of gonadal failure including post partum depression, premenstrual and perimenopausal mood swings and hot flushes. In light of the fact that interactions between the biological clock and the neuroendocrine hypothalamus seem to share similarities in rats and higher primates, the results gained in the current thesis could establish a fundamental hormone-dependent mechanism by which the biological clock functions. This, in turn, may offer new avenues to enhance the clinical management of the aforementioned symptoms.

MATERIALS AND METHODS

OBJECTIVE 1) Does the circadian clock, SCN, provides direct signals for neuroendocrine cells, including those producing GnRH and dopamine? A combination of anterograde, retrograde tracing and light and electron microscopic multiple label immunocytochemistry was carried out.

Animals

Ten, adult female Sprague-Dawley rats (250 - 280 g b. w.) were kept under standard laboratory conditions: tap water and standard rat chow *ad libitum*, 12 h light/dark cycle.

PHA-L injections

The projection field of SCN neurons was visualized by using PHA-L (2.5% in 10 mM PB, pH 7.8; Vector Laboratories, Burlingame, CA, USA) as an anterograde tracer. This was unilaterally applied with iontophoresis, via a glass micropipette (tip diameter 15 μm, 5 μA positive current applied every other 5 s for 15 min using a constant current source that is capable of generating up to 2,000 V, CS-3 Transcientic System, Canton, MA, USA) into different areas of the SCN (coordinates: A-P: -0.8 to -1.3 mm; L: 0.2 mm; V: 9.6 mm according to (Paxinos and Watson (84)).

Fluoro-gold (FG) injection

Simultaneously with the PHA-L injections, animals received a single intraperitoneal injection of FG (20mg/b.w.; Fluorochrome, INC., Englewood, CO) to label neurons that send projections to regions in the central nervous system that lack blood-brain barrier (85,86).

Fixation

Fifteen days after PHA-L/FG injections, rats were sacrificed under ether anesthesia by transaortic perfusion with 50 ml heparinized saline followed by 250 ml of fixative. The fixative consisted of 4% paraformaldehyde, 15% picric acid, and 0.2% glutaraldehyde in 0.1% phosphate buffer (PB), pH 7.4. The brains were dissected out and 3mm thick coronal blocks containing the hypothalamus were postfixed for an additional 1-2 hours in glutaraldehyde-free fixative.

Tissue preparation and immunostaining

Tissue blocks were rinsed in several changes of PB, and 50 μm vibratome (Lancer) sections were prepared and rinsed 4x 15 min in PB. Sections for electron microscopy were transferred into vials containing 0.5 ml of 10 % sucrose (in PB), and rapidly frozen by immersing the vial in liquid nitrogen to enhance antibody penetration. They were then thawed to room temperature, and repeatedly washed in PB. Subsequently, sections for both light and electron microscopy were treated with 1% sodium borohydride in PB for 10 min to eliminate unbound aldehydes from the tissue.

Immunostaining for PHA-L, FG and tyrosine hydroxylase (TH) or GnRH was carried out according to the following protocol: Incubation in biotinylated rabbit anti-PHA-L, 1:250 in PB containing 1% normal goat serum and 0.3% Triton X-100 for 48 h at 4°C. Following several washes in PB, sections were incubated in avidin-biotin-peroxidase, 1:500 in PB (ABC Kit, Vector Labs, Burlingame, CA), followed by a modified version of the Ni-DAB reaction (15 mg DAB, 0.12 mg glucose oxidase, 12 mg ammonium chloride, 600 μl 0.05 M nickel ammonium sulfate, and 600 μl 10% β-d-glucose in 30 ml PB for 5-10 min at room temperature; dark-blue reaction product) to visualize the tissue-bound peroxidase. After several rinses in PB, sections were further immunostained for FG. In this procedure, after a 48 hour (at 4°C) incubation in rabbit-anti-FG antiserum (Biogenesis, Inc., Franklin, MA) (1:5,000 in PB containing 0.1% sodium azide and 1% normal goat serum), sections were further processed in the secondary antibody (biotinylated goat-anti rabbit IgG, 1:250 in PB, Vector Labs, Burlingame, CA) for 2 h at room temperature, than rinsed in PB for 3x 10 min, and incubated for 2h at room temperature with ABC Elite, 1:250 in PB (ABC Elite Kit, Vector Labs, Burlingame, CA), followed by the above described Ni-DAB reaction. After several rinses in PB, every other section was placed on gelatin coated slides, dehydrated through increasing ethanol concentrations, and mounted with Permount. The remaining sections were further immunostained for TH or GnRH. In this procedure, after a 48 hour (at 4°C) incubation in either mouse-anti-TH antiserum (Incstar; 1:1,000 in PB containing 0.1% sodium azide and 1% normal horse serum) or in rabbit anti-GNRH antiserum, sections were incubated in the secondary antibody (goat-anti-mouse IgG), 1:50 in PB for 2h at room temperature, followed by peroxidase-anti-peroxidase (PAP): rabbit

PAP, 1:100 in PB. Between each incubation step, sections were rinsed for 3X15 min. in PB. In this case, the tissue bound peroxidase was visualized by a light brown DAB reaction (15 mg DAB, 165 µl 0.3% H_2O_2 in 30 ml PB, 5-10 min. at room temperature; brown reaction product). Following immunostaining of the third tissue antigen, sections were thoroughly rinsed in PB, placed on gelatin coated slides, dehydrated through increasing ethanol concentrations, and mounted with Permount. In control experiments, one or two primary antibodies were replaced with normal serum resulting in only single- or double immunolabeling.

For electron microscopic analysis, sections were processed the same way as for light microscopy, except the labeling of TH was carried out using 5 nm immunogold-conjugated goat anti-rabbit IgG (Polysciences, Warrington, PA) as secondary antiserum. Subsequently, sections were postosmicated (1% OsO_4 in PB) for 30 min, dehydrated through increasing ethanol concentrations (using 1% uranyl acetate in the 70% ethanol, 30 min) and flat embedded in Araldite between liquid release (Electron Microscopy Sciences, Fort Washington, PA) coated slides and coverslips, and placed in an oven to polymerize for 48 h at 60 °C. Flat embedded sections were fixed with a drop of embedding medium on the top of cylindrical araldite blocks and cured again for 48 h at 60°C. Then, blocks were trimmed using light micrographs as a guide in recognizing the selected retrogradely labeled cells and contacts. Ribbons of ultrathin sections (Reichert-Jung Ultramicrotome) were collected on Formvar-coated single slot grids, and examined using a Philips CM-10 electron microscope.

Semiquantitative ánalisys

To gain insight into the extent of colocalization of FG and TH, and to approximate the frequency of interconnections between SCN efferents and dopaminergic cells a semi-quantitative analysis was carried out manually, on light microscopic material from two animals, using every other section from the beginning of the third ventricle through hypothalamus up to the anterior part of the mammillary body. When assessing the size of the population of dopaminergic cells that are neuroendocrine, only cell bodies of TH-immunoreactive neurons were analyzed. Putative contacts between dark, PHA-L-immunoreactive axon terminals and anything other than cell bodies or proximal dendrites of the light brown TH-immunoreactive and/or FG labeled neurons were ignored. An axo-somatic or axo-dendritic contact was noted only if a bouton-like

structure was in close proximity to a cell body or dendrite and was found as a continuation of its axon by changing the focus plane.

OBJECTIVE 2) Can the IGL in the lateral geniculate body provide signals to neuroendocrine cells independent of the SCN? In addition t anterograde, retrograde tracing and light and electron microscopic multiple label immunocytochemistry, this study also employed acute axonal degeneration to label efferents of the retina.

Animals

Female Sprague-Dawley rats (250 - 280 g b. w.) were kept under standard laboratory conditions: tap water and standard rat chow *ad libitum*, 12 h light/dark cycle. Two sets of experiments were carried out on two groups of randomly selected females (the status of the estrus cycle was not determined). One group included animals (n=6) in which LGN efferents were labeled with *Phaseolus vulgaris* leucoagglutinin (PHA-L) and neuroendocrine cells with systemic fluorogold (FG) injections. In another group of rats (n=6), retrograde labeling of LGN neurons was carried out on enucleated animals by iontophoretic injections of FG into extrasuprachiasmatic regions of the hypothalamus. All the experimental procedures were approved by the Yale Animal Care Committee.

PHA-L injections

The projection field of LGN neurons was visualized by using PHA-L (2.5% in 10 mM PB, pH 7.8; Vector Laboratories, Burlingame, CA, USA) as an anterograde tracer. This was unilaterally applied by iontophoresis, via a glass micropipette (tip diameter 15 μm, 5 μA positive current applied every other 5 s for 15 min using a constant current source that is capable of generating up to 2,000 V, CS-3 Transcientics System, Canton, MA, USA) into different areas of the IGL (coordinates: A-P: -4.2 mm; L: 3.6 mm; V: 5.3 mm according to Paxinos and Watson (84)).

Fluoro-gold (FG) injection

Simultaneously with the PHA-L injections, animals received a single intraperitoneal injection of FG (20mg/kg b.w. in saline; Fluorochrome, Inc., Englewood, CO) to label neurons

that send projections to regions in the central nervous system that lack blood-brain barrier (85,86).

In a group of animals that were binocularly enucleated (see below), FG (2% FG in saline) was applied into extrasuprachiasmatic sites where LGN efferents contacted neuroendocrine cells (A-P: 0.0-1.3 mm; L: 0.2 mm; V: 9.4-8.8 mm according to Paxinos and Watson (84)). These FG injections were applied iontophoretically, using the same parameters as for the PHA-L experiments (see above).

Bilateral enucleation

In a group of animals, in parallel with the FG injections, both eyes of the animals were surgically removed under ketamine anesthesia.

Fixation and tissue preparation

Fifteen days after PHA-L/FG injections and 5 days after FG/enucleation, rats were sacrificed under metofane anesthesia by transaortic perfusion with 50 ml heparinized saline followed by 250 ml of fixative. The fixative consisted of 4% paraformaldehyde, 15% picric acid, and 0.2% glutaraldehyde in 0.1M phosphate buffer (PB), pH 7.4. The brains were dissected out and 3mm thick coronal blocks containing the diencephalon were postfixed for an additional 1-2 hours in glutaraldehyde-free fixative. Tissue blocks were rinsed in several changes of PB, and 50 μm vibratome (Lancer) sections were prepared and rinsed 4x 15 min in PB. Subsequently, sections for both light and electron microscopy were treated with 1% sodium borohydride in PB for 10 min to eliminate unbound aldehydes from the tissue.

Immunostaining

PHA-L/FG studies

Immunostaining for PHA-L, FG and tyrosine hydroxylase (TH) was carried out as follows. First, sections were incubated in biotinylated rabbit anti-PHA-L, 1:250 in PB containing 1% normal goat serum and 0.3% Triton X-100 for 48 h at 4°C. Following several washes in PB, sections were incubated in avidin-biotin-peroxidase, 1:500 in PB (ABC Kit,

Vector Labs, Burlingame, CA), followed by a modified version of the Ni-DAB reaction (15 mg DAB, 0.12 mg glucose oxidase, 12 mg ammonium chloride, 600 µl 0.05 M nickel ammonium sulfate, and 600 µl 10% β-d-glucose in 30 ml PB; dark-blue reaction product) to visualize the tissue-bound peroxidase. Then, sections were further immunostained for FG. In this procedure, after a 48 hour (at 4 °C) incubation in rabbit-anti-FG antiserum (Biogenesis, Inc., Franklin, MA) (1:5,000 in PB containing 0.1% sodium azide and 1% normal goat serum), sections were further processed in the secondary antibody (biotinylated goat-anti rabbit IgG, 1:250 in PB, Vector Labs, Burlingame, CA) for 2 h at room temperature, then rinsed in PB for 3x 10 min, and incubated for 2h at room temperature with ABC Elite, 1:250 in PB (ABC Elite Kit, Vector Labs, Burlingame, CA), followed by the above described Ni-DAB reaction. After several rinses in PB, every other section was placed on gelatin coated slides, dehydrated through increasing ethanol concentrations, and mounted with Permount. The remaining sections were further immunostained for TH. In this procedure, after a 48 hour (at 4°C) incubation in mouse-anti-TH antiserum (Chemicon, Temecula, CA; 1:1,000 in PB containing 0.1% sodium azide and 1% normal horse serum), sections were incubated in the secondary antibody (goat-anti-mouse IgG), 1:50 in PB for 2h at room temperature, followed by peroxidase-anti-peroxidase (PAP), rabbit PAP, 1:100 in PB. Between each incubation step, sections were rinsed for 3X15 min. in PB. In this case, the tissue bound peroxidase was visualized by a light brown DAB reaction (15 mg DAB, 165 µl 0.3% H_2O_2 in 30 ml PB, 5-10 min. at room temperature; brown reaction product). Following immunostaining of the third tissue antigen, sections were thoroughly rinsed in PB, placed on gelatin coated slides, dehydrated through increasing ethanol concentrations, and mounted with Permount. In control experiments, one or two primary antibodies were replaced with normal serum resulting in only single- or double immunolabeling.

For electron microscopic analysis, sections were processed the same way as for light microscopy, except the labeling of TH was carried out prior to PHA-L and FG immunostaining using 5 nm immunogold-conjugated goat anti-mouse IgG (Polysciences, Warrington, PA) as secondary antiserum. Subsequently, sections were postosmicated (1% OsO_4 in PB) for 30 min, dehydrated through increasing ethanol concentrations (using 1% uranyl acetate in the 70% ethanol, 30 min) and flat embedded in Araldite between liquid release (Electron Microscopy

Sciences, Fort Washington, PA) coated slides and coverslips, and placed in an oven to polymerize for 48 h at 60 °C. Flat embedded sections were fixed with a drop of embedding medium on the top of cylindrical araldite blocks and cured again for 48 h at 60 °C. Then, blocks were trimmed using light micrographs as a guide in recognizing the selected retrogradely labeled cells and contacts. Ribbons of ultrathin sections (Reichert-Jung Ultramicrotome) were collected on Formvar-coated single slot grids, and examined using a Philips CM-10 electron microscope.

FG/enucleation studies

In this case, only single labeling for FG was carried out as described above using the polyclonal antiserum against FG and an ABC procedure followed by a DAB reaction (see above).

OBJECTIVE 3) Can gonadal signals be integrated into the hypothalamo-pituitary axis outside of the hypothalamus, in the IGL? To test this hypothesis, in situ hybridization hystochemistry was carried out for etsrogen receptor beta (ERβ) and progesterone receptor (PR).

Animals and Tissue Collection

Intact female and male Sprague-Dawley rats (190-200g; n=6/group; Taconic, Germantown, NY) were housed in the animal care facility (AAALAC certified) with a 12-h light, 12-h dark photoperiod and free access to tap water and rodent chow. Animals were exposed to a lethal dose of CO2 and the brains frozen on dry ice and stored at -80 °C.

***In situ* Hybridization**

In order to investigate the distribution of ER-β and PR mRNA with in situ hybridization, specific cRNA probes for each receptor was used. Previously, two fragments (ER-β-558, bases 52-610 and ER-β-285, bases 1809-2094) of the rat ER-β cDNA (87) were subcloned and it was found that an ER-β-285/558 cocktail of cRNA probes gave good hybridization signal that was specific for ER-β mRNA (87). A fragment (bases 2177-2992) of the rat PR cDNA was amplified using PCR and the rPR-2 plasmid (87,88) as a template. The fragment was subcloned into a pCRII plasmid (Invitrogen, San Diego, CA), excised with EcoR I and then subcloned into the

EcoR I site of a pBluescript plasmid (Stratagene, La Jolla, CA). The resulting plasmid (PR-815) contained an 815 bp fragment of the rat PR cDNA. The PR-815 plasmid was linearized with Hind III (sense; control) or BamH I (antisense) and used to generate S^{35}-UTP labeled cRNA probes for *in situ* hybridization.

The in situ hybridization methodology utilized for these studies has been described previously (87,88). Two sets of adjacent 20 μm cryostat sections were collected on gelatin-coated slides, dried and then stored at -80 °C in desiccated boxes. At the time of processing, the slide were warmed to room temperature, postfixed in paraformaldehyde, treated with acetic anhydride and then delipidated and dehydrated. Processed section-mounted slides were hybridized with 200 ml of an antisense or sense (control) riboprobes (ER-β-285/558, PR-815; 8-12 x106 DPM/ slide) -50-% formamide hybridization mix and incubated overnight at 55 C in an open-air humidified slide chamber. In the morning, the slides were immersed in 2xSSC (0.3 M NaCl, 0.03 M sodium citrate; pH 7.0) / 10 mM DTT, treated with RNase A (20 mg/ml) and washed (2X 30 min at 65 C ER-β-285/558 or 68 C PR-815) in 0.1xSSC to remove nonspecific label. After dehydration, the slides were apposed to BioMax (BMR-1; Kodak) x-ray film for 7 days and then dipped in NTB2 nuclear emulsion (Eastman Kodak; diluted 1:1 with 600 mM ammonium acetate). The slides were exposed for 30 days in light-tight black desiccated boxes, photographically processed, stained in cresyl violet and coverslipped. The slides from all animals were hybridized, washed, exposed and photographically processed together to eliminate differences due to interassay variation in conditions.

Evaluation

Section-mounted slides were viewed with high magnification to determine the cellular distribution of hybridization signal for ER-β or PR mRNA and to verify that silver grains were concentrated over cells. Cells with a concentration (> 5X radioactivity in surrounding areas) of silver grains were considered labeled.

OBJECTIVE 4) Is the development of the biological clock under the control of gonadal steroids? To test this hypothesis, in this experiment, immunocytochemistry for aromatase, the key enzyme in sexual differentiation, was carried out on different areas of the developing rat. To

confirm the existence of aromatase in these areas, a biochemical assay for aromatase activity was also done.

Immunocytochemistry

Brains from male and female Sprague-Dawley rats killed at embryonic day (E)14 (n=10), E18 (n=10), postnatal day (P)0 (n=10), P5 (n=10), P10 (n=10), and P20 (n=10) were processed for *immunocytochemistry*. Embryonic tissue was immersion fixed using 4% paraformaldehyde, while postnatal animals were perfused transcardially with the same solution. Embryonic brains were cryosectioned and mounted on gelatin coated slides. Postnatal tissue was vibratome sectioned and free floated. Immunolabeling for aromatase was carried out using two different antisera raised against either a synthetic 20 amino acid sequence of aromatase (89,90) or human placental aromatase (91-93). After incubation with either of the primary antisera (1:5000 in both cases) for 48 h at 4 °C, sections were processed with a biotinylated secondary antiserum (anti-rabbit IgG; 1:250; Vector Labs., Burlingame, CA) for 2 hours at room temperature followed by incubation in Avidin DH plus biotinylated peroxidase complex (1:50) for 2h at room temperature. Tissue-bound peroxidase was visualized using a nickel ammonium sulfate-intensified diaminobenzidine (DAB) reaction (15 mg DAB, 0.12 mg glucose oxidase, 12 mg ammonium chloride, 600 µl 0.05M nickel ammonium sulfate, and 600 µl 10% β-d-glucose in 30 ml phosphate buffer (PB) for 5-10 min. at room temperature; dark-blue reaction product). In control experiments in which the primary antiserum was replaced with normal serum, no immunostaining could be detected.

Sections were analyzed using a bright field microscope. Cell bodies, proximal dendrites and distal processes were analyzed by 100X magnification (oil immersion). A neuronal cell body was recognized if the cell nucleus and nucleolus could clearly be identified and its shape fulfilled the criteria of a neuron (shape of cell and nucleus; ratio of cytoplasm and nucleus; process arborization and shape) and not of an astrocyte, oligodendrocyte or microglia. Axons were recognized if they were present in fiber bundles (for example spinotrigeminal tract), the transection of the path did not result in donut-like appearance of immunolabeling (myelin) in processes, in the target region of that tract, arborization of axons and bouton formation could be detected. Cell abundance and surface density of immunolabeling was assessed by an Image-1/AT image processor (Universal Imaging Corporation, West Chester, PA) using an Olympus IMT-2

inverted microscope with bright field optics (Olympus Corporation, Lake Success, New York) and a Hamamatsu CCD camera (Hamamatsu Photonics, Hamamatsu, Japan) (94). The number of labeled cells or total surface covered by labeled axons was assessed in different brain nuclei and fiber pathways, within a test region measuring 10^{-5} μm^2. After collecting the data, the density of aromatase cells and processes was expressed in percentage of the measured surface and described as low (+; 1-25%), moderate (++; 25-50%), high (+++, 50-75%) and very high (++++; 75-100%).

Aromatase assay

In P10 animals, aromatase activity was measured by a 3H-release assay, in which [1β-^{3}H] testosterone was used as substrate. P10 rats of both sexes were ether anaesthetized and then decapitated. Brains were dissected to yield a pooled sample containing the entire hypothalamus, preoptic area, and amygdala (positive control), a cerebellar sample (negative control), and a sample containing the spinotrigeminal tract. Four animals were pooled for each of the five analysis (n=5). Tissues were homogenized in sodium phosphate with 1ml buffer/100ng of tissue. Aliquots of tissue homogenates were incubated for 4h at 37 °C with 0.2 ml of an NADPH generating system (4mM ATP, 4mM NADP, 10mM glucose-6-phosphate and 4I.U. of glucose-6-phosphate dehydrogenase) and 50 pmols of [1β-^{3}H] testosterone. At hours 0, 1, 2, and 4, 0.4 ml of tissue homogenates were removed from the sample and analyzed for dpm after chloroform and charcoal treatments. After assessing the dpm count of 50 pmols of [1β-^{3}H] testosterone, and those of the boiled and 0h controls , the collected dpm counts of the different experimental tissues were translated to fmol values.

OBJECTIVE 5) Is the SCN input to GnRH cells gender specific? To addres this issue, quantitative analysis of the vasoactive intestinal polipeptide (VIP)-containing input of GnRH neurons was assessed in male and female rats. This input has previously been shown to originate in the SCN (95).

Animals

Adult male (n=5) and cycling adult female (n=5) Sprague-Dawley rats (200-250 g b.w.) were used in this experiment. Animals were kept under standard laboratory conditions, with tap water and regular rat chow available *ad libitum*, in a 12-h light, 12-h dark cycle. Cycling female

rats were used after demonstrating at least two, consecutive four-day ovarian cycles assessed by vaginal smears, and were sacrificed in the morning of metestrous (10.00 AM). Males were killed at the same hour of the day. Rats were killed under ether anesthesia, by transaortic perfusion with 50 ml of isotonic saline followed by 250 ml of fixative. The fixative consisted of 4% paraformaldehyde and 15% picric acid in 0.1M phosphate buffer (PB, pH 7.4). The brains were removed from the skull and 3 mm thick coronal blocks containing the hypothalamus were cut and postfixed for an additional 2 h. Tissue blocks were rinsed in several changes of PB and 40 μm sections were cut on a vibratome (Lancer) and rinsed in PB.

Immunostaining

Light microscopic double immunostaining for VIP and GnRH was carried out according to the following protocol. Sections were incubated with VIP antiserum (raised in mouse; 1:5000 in PB containing 1% normal goat serum and 0.3% triton-X-100; INCSTAR Cooperation, Stillwater, MN) for 48 h at 4 °C. After several washes with PB, sections were incubated in the secondary antibody (biotinylated horse anti-mouse IgG; 1:250 in PB; Vector Laboratories, Burlingame, CA) for 2 h at room temperature, then rinsed in PB three times for 10 minutes each time, and incubated for 2 h at room temperature with avidin-biotin-peroxidase (ABC, 1:250 in PB; ABC Elite Kit, Vector Labs). The immunoreaction was visualized with a modified version of nickel-diamidobenzide (Ni-DAB) reaction (15 mg DAB, 0.12 mg glucose oxidase, 12 mg ammonium chloride, 600 μl 0.05 M nickel ammonium sulfate, and 600 μl 10% β-d-glucose in 30 ml PB) for 10-30 min at room temperature resulting in a dark blue reaction product. After several rinses in PB, the sections were incubated in rabbit anti-GnRH antiserum (1:1000 in PB containing 0.1% sodium azide; Incstar Co., Stillwater, MS) for 48 h at 4 °C, followed by a secondary antibody (goat anti-rabbit IgG; 1:50 in PB), and rabbit peroxidase-anti-peroxidase (PAP; 1:100 in PB) both for 2 h at room temperature. Between each incubation step, the sections were rinsed three times for 15 min with PB. The tissue-bound peroxidase was visualized with a DAB reaction (15 mg DAB and 165 μl 0.3% H_2O_2 in 30 ml PB) for 10 min at room temperature, resulting in a light brown reaction product. After immunostaining, the sections were thoroughly rinsed in PB, mounted on gelatin-coated slides, dehydrated through graded series of ethanol and xylene, and cover slipped using Permount. In control double staining experiments, in which one

of the primary antibodies was replaced with normal serum, only one single immunostaining was detected.

Semi-quantitative analysis

To assess the frequency of connections between VIP-immunoreactive axons and GnRH cells a semi-quantitative analysis was carried out manually on light microscopic material on five animals of each sex. Every other section from the beginning of the medial septum through the diagonal band and medial preoptic area up to the anterior part of the SCN was used for the analysis. Putative contacts between dark blue, VIP-immunoreactive axon terminals and anything other than cell bodies or proximal dendrites of the light brown GnRH-immunoreactive neurons were ignored. Using 100x objective with oil-immersion, an axo-somatic or axo-dendritic contact was noted only if a VIP-immunoreactive bouton-like structure was in close proximity to a cell body or dendrite and was found as a continuation of its axon by changing the focus plane. The following parameters were assessed in each animal: the number of GnRH neurons and the percentile of GnRH neurons contacted by VIP axons, and the mean number of VIP-immunoreactive boutons on these VIP-contacted GnRH cells.

The analysis of variance test demonstrated a significant non-homogeneity of variance between groups. Therefore, the Tukey/Os pair-wise test was selected to compare mean values between groups. A level of confidence of $p<0.05$ in a two tailed test was adopted for statistical significance.

RESULTS

OBJECTIVE 1) Does the circadian clock, SCN, provides direct signals for neuroendocrine cells, including those producing GnRH and dopamine

Single labeled profiles

PHA-L injection and immunolabeling

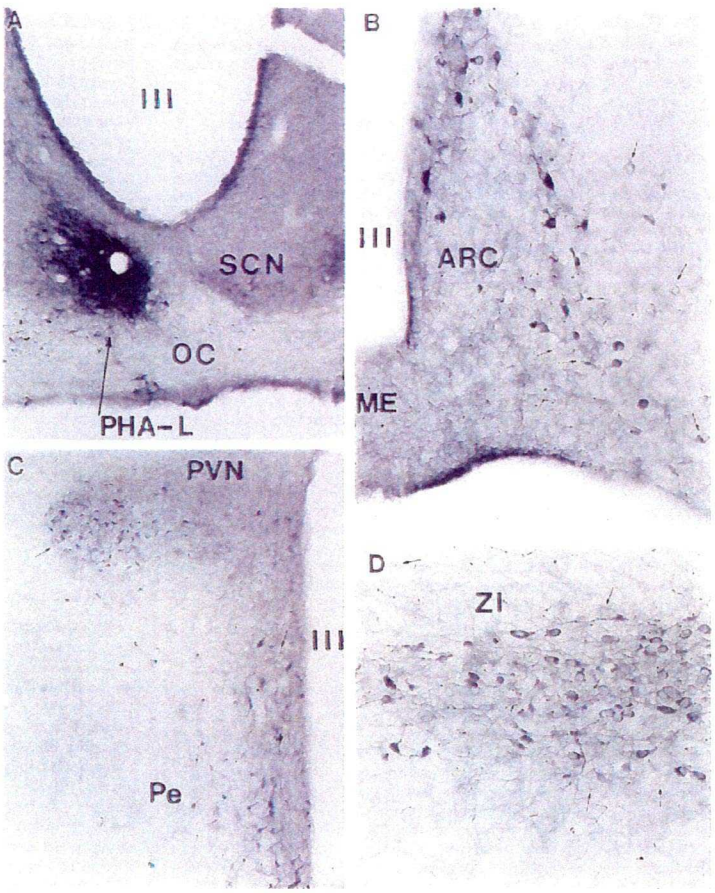

Ten animals received PHA-L injections. Histological examination showed that four injections were restricted within the boundaries of the SCN, while the rest involved surrounding areas as well. These latter animals were excluded from this study.

All four injections were placed in the ventral aspects of the SCN (Fig. 1A). The number of labeled neurons was between 200 and 250 representing approximately 2% of the SCN neuron population. Labeled axon terminals were seen in each region of the SCN. The majority of PHA-L-labeled fibers were seen to leave the SCN in the dorsal direction. Few axons were found to run

Fig. 1

Panel A shows a typical PHA-L injection site in the suprachiasmatic nucleus (SCN). PHA-L immunoreactive cell bodies are limited to the boundaries of the SCN, and labeled processes can be seen leaving the nucleus dorsally as well as ventrally joining the optic tract (OC). Panels B-D are light micrographs double immunostained for TH and FG. They illustrate the distribution pattern of TH labeled dopamine cells (light brown profiles) and retrogradely labeled, FG-containing neurons (arrows) within the arcuate nucleus (ARC; panel B), paraventricular (PVN) and periventricular (Pe) nuclei (panel C) and in the zona incerta (ZI; panel D). Note that the only area where colocalization of TH and FG clearly cannot be seen at this magnification (original magnifications of panels B and D:X20, C:X10) is the zona incerta (panel D). In the arcuate nucleus and periventricular areas the number of TH-immunoreactive neurons which also expressed FG labeling was high. Note the dense TH immunolabeling in axons of the external layer of the median eminence (ME) on panel B. To see high power magnification of retrogradely labeled dopamine cells, see Fig. 2. III: third ventricle. Original magnification of panel A: X10.

towards and through the contralateral SCN or the ipsilateral optic tract. Sections taken from the diencephalon and adjacent areas showed that anterogradely labeled axons and axon terminals reached ventral aspects of the lateral septum, medial septum, bed nucleus of the stria terminalis medial preoptic area, anteroventral periventricular nucleus, medial preoptic nucleus periventricular region, parvicellular region of the paraventricular nucleus, subparaventricular zone, retrochiasmatic area, anterior hypothalamic nucleus, supraoptic decussation, ventrolateral aspects of the ventromedial hypothalamus, the cell-sparse zone between the ventromedial nucleus and the arcuate nucleus, dorsomedial hypothalamic nucleus, and zona incerta. Anterogradely labeled processes were also detected in the optic tract posterior to the injection site, and, in the intergeniculate leaflet of the ventrolateral geniculate body. The most abundant network of labeled fibers was detected in the subparaventricular zone while, the fewest were found in the zona incerta. While the predominant labeling was observed in the ipsilateral side, some axons were detected in contralateral areas as well.

FG immunolabeling

FG-immunopositive cell bodies and dendrites could be seen throughout the hypothalamus. Retrogradely labeled cells were abundant in the medial septum, medial preoptic area, organum vasculosum of laminae terminalis, diagonal band of Broca, supraoptic and paraventricular nuclei, arcuate nucleus, in the area between the arcuate nucleus and ventrolateral parts of the ventromedial nucleus, and in the zona incerta (see Fig. 1B-D). Fewer cells could be seen in the periventricular area, including subparaventricular zone and retrochiasmatic area, and in the lateral hypothalamus. No labeled neurons were detected in the suprachiasmatic nucleus. The distribution of retrogradely labeled hypothalamic cells corresponded to earlier descriptions (96).

FG immunolabeling resembled that of horseradish peroxidase labeling whereby the retrogradely transported peroxidase is confined to small cytoplasmic granules (see Figs 1-3). Electron microscopic analysis indicated that the FG immunostaining was associated with lysosome-like structures (Fig. 3).

TH immunostaining

Immunolabeling for *TH* resulted in extensive staining throughout the hypothalamus (Fig. 1B-D). Labeled cell bodies and dendrites were found in the anteroventral periventricular nucleus, medial preoptic area, periventricular area, parvocellular division of the paraventricular nucleus, anterior hypothalamus, arcuate nucleus and zona incerta. Axonal processes were abundant in most of the hypothalamic nuclei. The median eminence contained abundant network of TH-immunoreactive axonal processes in both its internal and external division (Fig. 1B). Immunolabeled processes were also detected in the organum vasculosum of laminae terminalis and subfornical organ. The appearance of TH-containing profiles in this experiment was in accordance with previous reports (48,97-99).

GnRH immunostaining

GnRH-immunoreactive cell bodies were distributed throughout the medial septum, diagonal band of Broca and medial preoptic area. Immunolabeled axonal processes were found in different parts of the hypothalamus, but were most abundant in the external layer of the median eminence.

Double labeled profiles

FG-TH double labeling

The granular appearance of FG immunoreactivity allowed for the labeling of cytoplasmic TH. In all of the hypothalamic areas where TH-immunoreactivity was detected, retrogradely transported FG was detected in sub-population of dopamine (TH) neurons (Figs. 1B-D and 2D, E). The highest incidence of double labeled cells was found in the arcuate nucleus (A 12 dopaminergic cell group), where out of 2593 TH-immunoreactive cells 2083 (80%) were also immunolabeled for fluorogold. In the periventricular area (A 12), 1442 TH-immunoreactive cells were analyzed of which 453 (31%) were retrogradely labeled. In the preoptic area (A 14), 42% (349/833) of TH-immunoreactive cells were FG-immunopositive as well. In the zona incerta, no retrogradely labeled dopamine cells were detected, while numerous nearby neurons contained FG (Fig. 1D). The extent of colocalization of FG and TH in this study corresponds to earlier descriptions of neuroendocrine dopaminergic cells of the hypothalamus (47,97,100).

PHA-L-FG double labeling

PHA-L immunoreactive dark blue fibers were detected in several regions that contained retrogradely labeled FG-immunoreactive neurons. These regions included the medial septum, medial preoptic area, periventricular areas, the subparaventricular zone just adjacent to the injection site, and a region between the arcuate and ventromedial nuclei. In these regions, PHA-L-labeled SCN efferents could be frequently found in close proximity to FG-labeled cell bodies

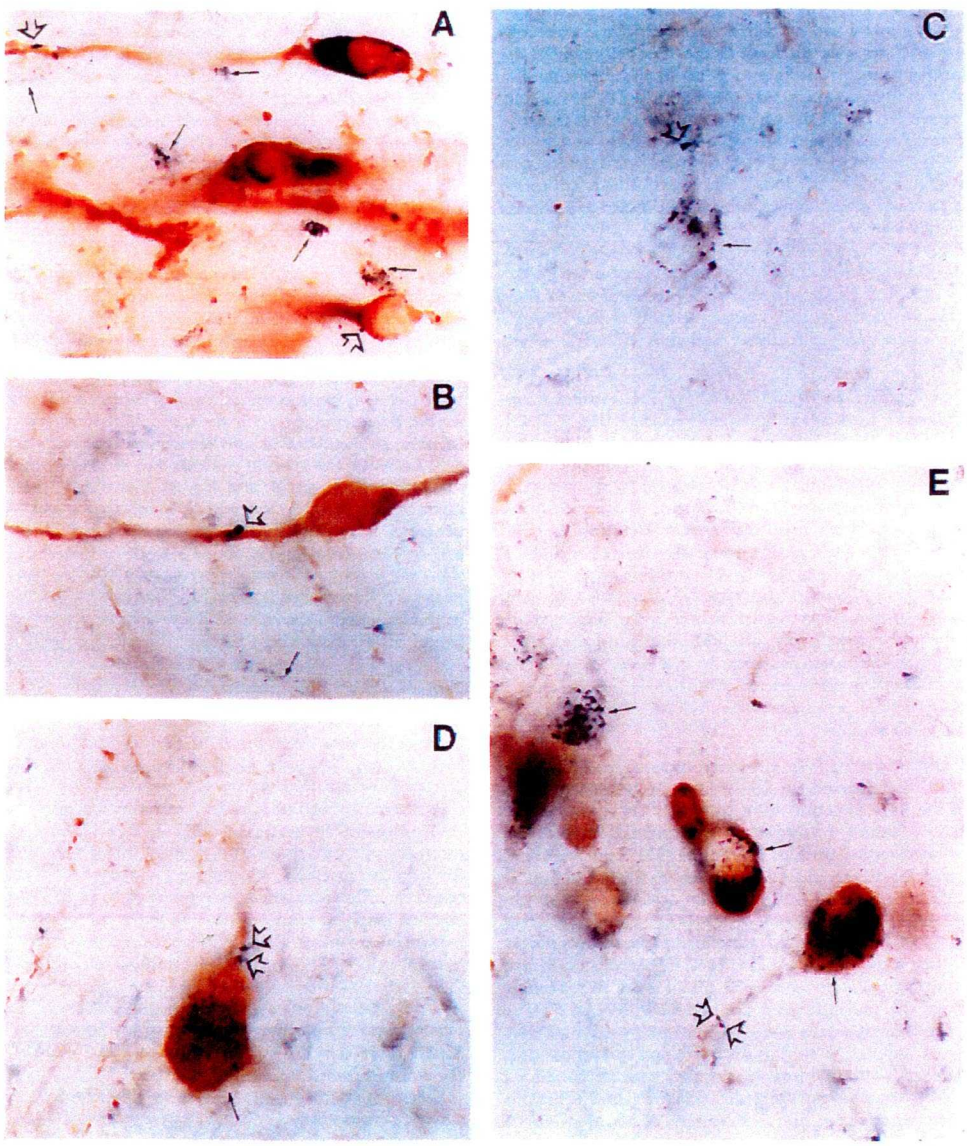

Fig. 2 Panels A-B: Light micrographs taken of putative connections between SCN efferents (PHAL-immunoreactive axon terminals; open arrows) and non-neuroendocrine (FG-negative) dopamine cells in the periventricular area. Panel C is a light micrograph illustrating a putative connection between a PHA-L -immunoreactive axon terminal (open arrow) and a non-dopaminergic, retrogradely labeled cell in the subparaventricular area. Panels D and E show retrogradely labeled (FG granules) dopamine cells (TH-immunoreactive) contacted by PHA-L-containing putative axon terminals (open arrows) in the anteroventral periventricular nucleus (D)and periventricular area (E). On panel E, both dopamine-containing and neurochemically un identified retrogradely labeled neurons can be seen. On panels A-E, neuroendocrine cells and profiles (FG immunolabeling alone) are indicated by small arrows. Original magnifications of panels A-E: X100.

and proximal dendrites (Fig. 2C). While quantitative analysis could not be carried out in this material, the frequency of these connections was highest in the medial septum-diagonal band-medial preoptic area axis and in the cell-sparse zone between the arcuate and ventromedial

nuclei. Fewer connections were found in the periventricular area and parvicellular division of the paraventricular nucleus. The vast majority of the putative connections were observed in the side ipsilateral to the injection, although, few connections were seen on the contralateral side as well. PHA-L immunoreactive fibers could not be detected in the organum vasculosum laminae terminalis, supraoptic nucleus, magnocellular division of the paraventricular nucleus, and in the arcuate nucleus where the highest number of retrogradely labeled neurons could be seen.

PHA-L-TH double labeling

PHA-L immunoreactive fibers were seen in close apposition to TH-immunolabeled cell within the medial preoptic area, anteroventral periventricular area, periventricular and retrochiasmatic regions and in an area between the arcuate nucleus and the ventromedial nucleus (Fig. 2A, B and Fig. 3) The majority of the appositions occurred between PHA-L-containing axons and the proximal dendrites of TH cells (Fig. 2A-B). However, axo-somatic connections could also be detected (Fig 3). In this case, again, connections between SCN efferents and dopamine cells were predominantly seen on the side ipsilateral to the injection. However, in few instances they were also found in the contralateral side.

PHA-L-GnRH double labeling

In the medial septum-diagonal band-medial preoptic area regions numerous PHA-L-immunolabeled SCN efferents were found in close proximity to GnRH-containing perikarya. Electron microscopic analysis of this material revealed symmetrical synaptic contacts between GnRH perikarya and proximal dendrites and PHA-L-immunolabeled axon terminals.

Triple labeled cells

In the hypothalamic regions, see above, where dopamine cells were detected to be retrogradely labeled, dark blue PHA-L boutons were found in contact with light brown TH-immunoreactive cell bodies and proximal dendrites-containing retrogradely transported dark blue FG-immunopositive granules (Fig. 2D, E). In a light microscopic semiquantitative analysis it was found that in the arcuate nucleus, where the majority of TH-immunoreactive cells were retrogradely labeled, out of 2083 neuroendocrine dopamine cells, 145 (7%) were contacted by PHA-L-immunoreactive, SCN efferents. In the periventricular area, 5% (27/453) of

neuroendocrine- and 10% (93/998) of the non-neuroendocrine dopamine cells were targeted by SCN efferents. In the preoptic area, PHA-L immunoreactive axon terminals were in close proximity to 6% (21/349) of neuroendocrine and 7% (34/484) of non-neuroendocrine dopamine cells.

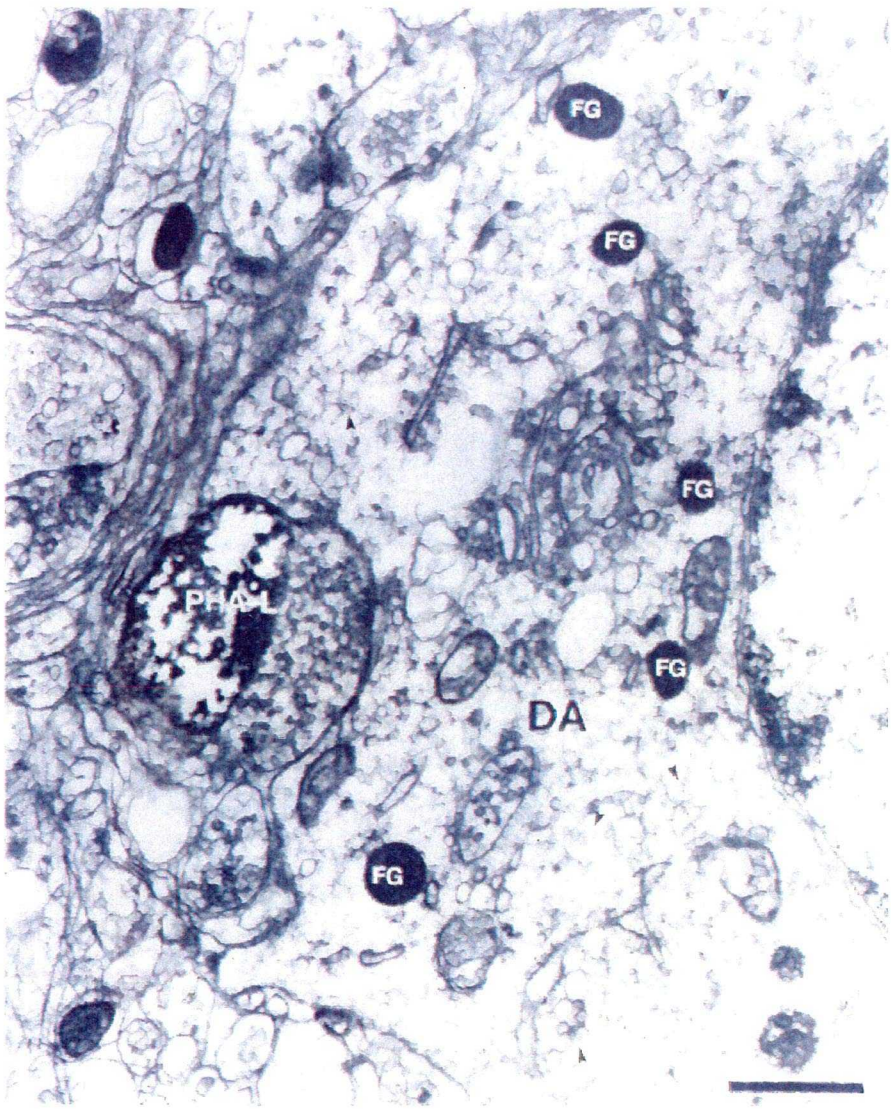

Fig. 3 Electron micrograph taken of the arcuate nucleus from the material triple immunolabeled for PHA-L, TH (arrowheads point to immunogold) and FG (arrows). The PHA-L-immunoreactive bouton is in close apposition to an unidentified axon terminal. Both exhibit membrane specializations resembling symmetrical dopaminergic (DA) soma. Bar scale: 1µm.

Electron microscopic analysis of this material revealed synaptic connections between PHA-L-immunoreactive axon terminals and retrogradely labeled TH cells (Fig. 3). The synaptic membrane specializations seemed to be symmetrical (Fig. 3).

OBJECTIVE 2) Can the IGL in the lateral geniculate body provide signals to neuroendocrine cells independent of the SCN?

PHA-L/FG/TH labeling

PHA-L injection and immunolabeling

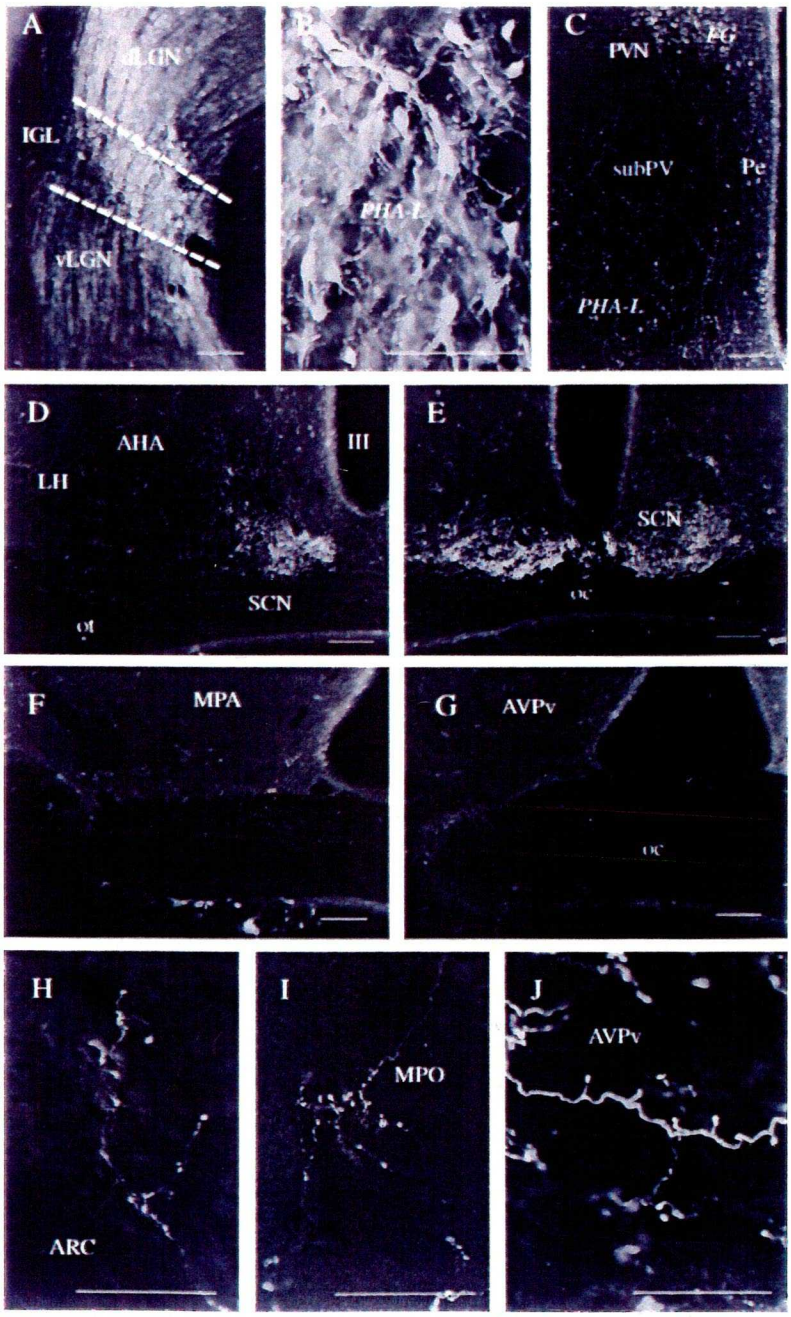

Six animals received PHA-L injections. Three of these injections were placed predominantly in the IGL as revealed by immunolabeling for PHA-L. Only tissue from these latter animals were fully processed according to the protocol.

Labeled perikarya were most abundant in the IGL, while PHA-L immunoreactive cells were also found in the adjacent areas of both the ventral (v) and dorsal (d) LGN (Fig. 4A&B). Labeled axons and axon terminals were detected in all parts of the LGN. In accordance with the labeled cell bodies, LGN efferents were observed in all previously reported projection sites of these nuclei, including the superior colliculus, posterior

Fig. 4 **A** and **B:** a typical injection site of **PHA-L**, in the LGN. **B:** is a high power magnification of the IGL area indicated on panel **A**. **C-G:** anterogradely labeled LGN efferents in the subparaventricular region (**subPV**; **C**), lateral hypothalamus (**LH**), periventricular area (**Pe**) and posterior **SCN** (**D**), anterior SCN (**E**) in the medial preoptic area (**MPO**; **F**) and in the anteroventral periventricular nucleus (**AVPv**; **G**). Labeled processes are also visible in the optic tract (**D**) and chiasm (**E-G**). **H-J**: high power light micrographs showing axon arborizations and axon terminals in the posterior arcuate nucleus (**ARC**; **H**), medial preoptic area (**MPO**; **I**) and in the **AVPv** (**J**). Scale bars represent 100 μm (**A-C; H-J**) and 300 μm (**D-G**).

commissure, and contralateral LGN. This study focused on the hypothalamic projection sites.

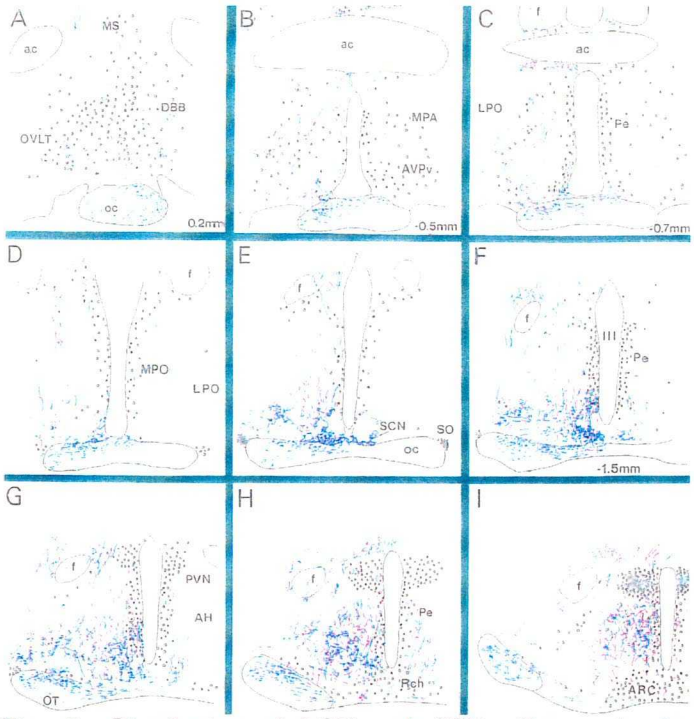

Fig. 5 Distribution of LGN and SCN efferents in the hypothalamus. Camera lucida drawings after immunostaining for PHA-L filled, LGN efferents (blue processes). Red processes represent PHA-L-labeled SCN efferents. Circles represent neuroendocrine cells, black filled circles are neuroendocrine cells that were TH-immunoreactive.

Sections taken from the diencephalon and adjacent forebrain areas showed that anterogradely labeled axons and axon terminals reached ventral aspects of the lateral and medial septal nuclei, diagonal band of Broca, bed nucleus of the stria terminalis, medial preoptic area (MPO), anteroventral periventricular nucleus (AVPv), medial preoptic nucleus periventricular region, parvicellular region of the paraventricular nucleus, subparaventricular zone, retrochiasmatic area, anterior hypothalamic nucleus, supraoptic decussation, suprachiasmatic nucleus, dorsomedial nucleus, ventrolateral aspects of the ventromedial nucleus and the cell sparse zone between the arcuate and ventromedial nuclei (Fig. 4C-H; Fig. 5). LGN efferents could also be detected in the ipsilateral optic tract and in both the ipsi and contralateral optic nerve (Fig. 4D&A). The most abundant network of labeled fibers could be seen in the ventral aspects of the SCN and the subparaventricular zone. No labeled processes could be detected in the median eminence, organum vasculosum laminae terminalis, and, only trespassing axons were found within the core of the arcuate nucleus and the magnocellular region of the paraventricular nucleus. While most of the labeling was observed in the ipsilateral side, some axons were detected in contralateral areas as well. Contralateral innervation was the most pronounced in the SCN and the subparaventricular area. In the case of the SCN, collaterals from the same axon could frequently be followed to both the ipsi and contralateral SCN.

In an attempt to compare the distribution pattern of SCN and IGL efferents in the hypothalamus, we analyzed serial vibratome sections immunostained for PHA-L from animals that received the tracer in the IGL (present studies) and in the SCN (a previous experiment; see

101). Upon superimposing camera lucida drawings from the two experiments, it could be seen that the projection field of IGL efferents within the hypothalamus almost completely overlapped that of the SCN (Fig. 5). Also note that while a quantitative analysis could not be carried out, the extent of the IGL innervation of different hypothalamic nuclei seemed to be comparable to that of the SCN.

FG immunolabeling

FG-immunopositive cell bodies and dendrites could be seen throughout the hypothalamus. Retrogradely labeled cells were abundant in the medial septum, medial preoptic area, organum vasculosum of laminae terminalis, diagonal band of Broca, supraoptic and paraventricular nuclei, arcuate nucleus, in the area between the arcuate nucleus and ventrolateral parts of the ventromedial nucleus, and in the zona incerta. Fewer cells could be seen in the periventricular area, including the subparaventricular zone and retrochiasmatic area, and in the lateral hypothalamus. No labeled neurons were detected in the SCN or IGL. The distribution of retrogradely labeled hypothalamic cells corresponded to earlier descriptions (85,101). In accordance with previous studies (102), the intraperitoneal administration of FG resulted in a different appearance of the immunoperoxidase reaction product in cells than resulted from the iontophoretic application (see below). FG labeling in the former had a granular appearance, whereas, in the latter, FG labeling was homogeneously distributed in the IGL cells. It is likely that this difference is the result of the low levels of FG in the circulation in contrast to the concentration given for iontophoretic application.

TH immunostaining

Immunolabeling for *TH* resulted in extensive staining throughout the hypothalamus. Labeled cell bodies and dendrites were found in the AVPv, MPO, periventricular area, parvocellular division of the paraventricular nucleus, anterior hypothalamus, arcuate nucleus and zona incerta. Axonal processes were abundant in most of the hypothalamic nuclei. The median eminence contained an abundant network of TH-immunoreactive axonal processes in both its internal and external division. The appearance of TH-containing profiles in this experiment was in accordance with previous reports (48,49,98,99).

FG-TH double labeling

The granular appearance of FG immunoreactivity permitted the detection of the labeling of cytoplasmic TH. In all of the hypothalamic areas where TH-immunoreactivity was detected, retrogradely transported FG was detected in a subpopulation of TH-immunoreactive, putative dopamine neurons (Fig. 5 and Fig. 6E-G2). The highest incidence of double labeled cells was found in the arcuate nucleus (A 12 dopaminergic cell group) followed by the periventricular area and the preoptic area (A14 dopaminergic cell group). In the zona incerta, no retrogradely labeled dopamine cells were detected, while numerous neurons nearby contained FG. The extent of colocalization of FG and TH in this study corresponds to earlier descriptions of neuroendocrine dopaminergic cells of the hypothalamus (47,49,100,101).

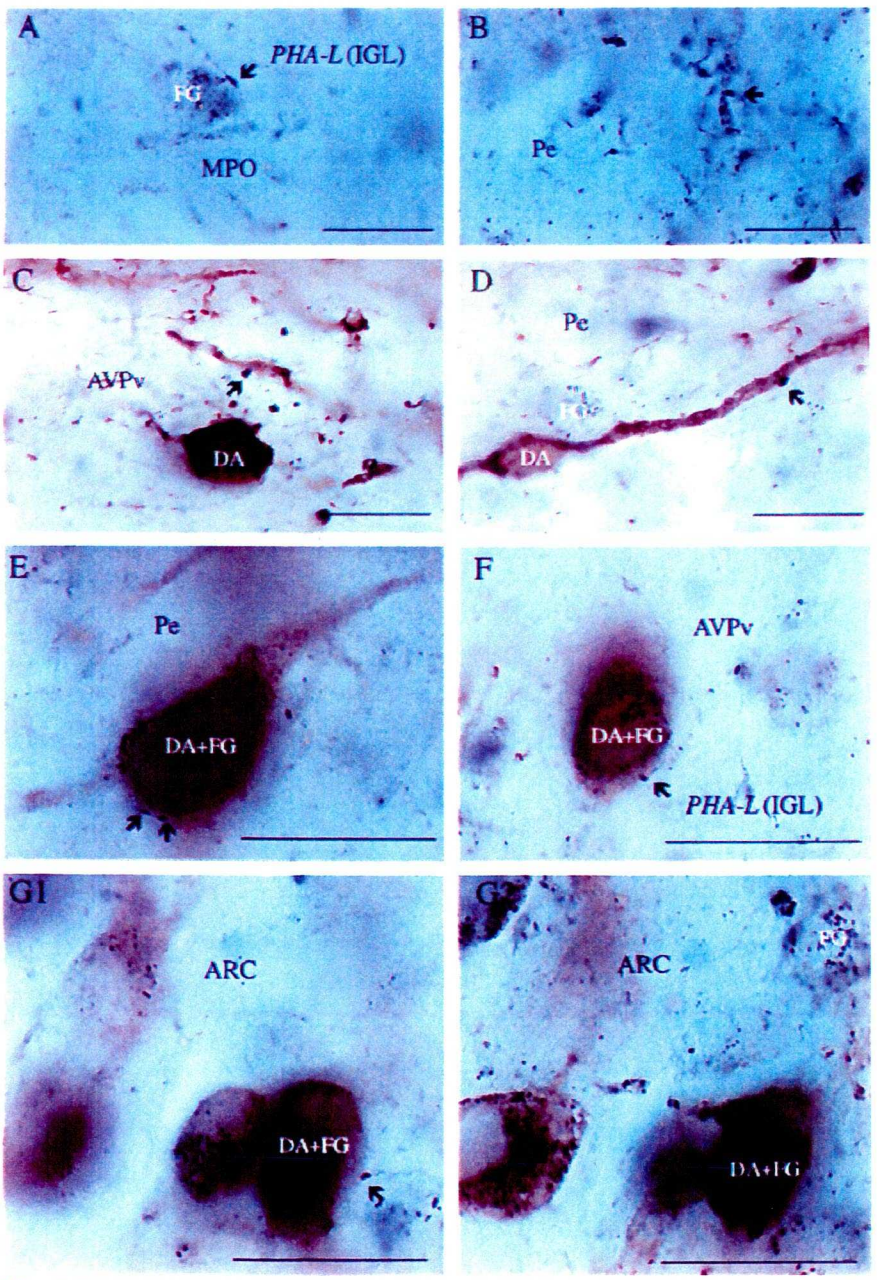

PHA-L-FG double labeling

PHA-L immunoreactive dark blue fibers were

Fig. 6 LGN efferents contacting hypothalamic neuroendocrine and/or dopamine cells. **A-B**: Dark blue boutons originating in the LGN in close proximity to an FG-containing perikaryon and dendritic process of the MPO and the Pe, respectively. **C and D**: Putative connections between IGL efferents (PHAL-immunoreactive axon terminals; arrows) and non-neuroendocrine (FG-negative) dopamine cells in the AVPv and Pe. **E-G1** show retrogradely labeled (FG granules) dopamine cells (TH-immunoreactive) contacted by PHA-L-containing putative axon terminals (arrows) in the **Pe (E)**, **AVPv (F)** and the lateral aspects of the ARC (**G1**). **G2** shows the same cells as **G1** but at a different focus plane to enhance the visibility of FG-immunoreactive cytoplasmic inclusions. Bar scales represent 10 μm.

detected in several regions that contained retrogradely labeled FG-immunopositive neurons (Fig. 5). These regions included the medial septum, MPO, periventricular areas, the subparaventricular zone, and a region between the arcuate and ventromedial nuclei (Fig. 5). In these regions, PHA-L-labeled LGN efferents could often be found in close proximity to distinct populations of FG-labeled cell bodies and proximal dendrites (Fig. 6A&B). Similar to the experience with SCN efferents (101), the frequency of these connections was highest in periventricular areas, including the anteroventral periventricular nucleus, and in the cell-sparse zone between the arcuate and ventromedial nuclei. Fewer connections were found in the parvicellular division of the paraventricular nucleus. The putative connections were observed predominantly in the side ipsilateral to the injection, although, a few connections were seen on the contralateral side as well.

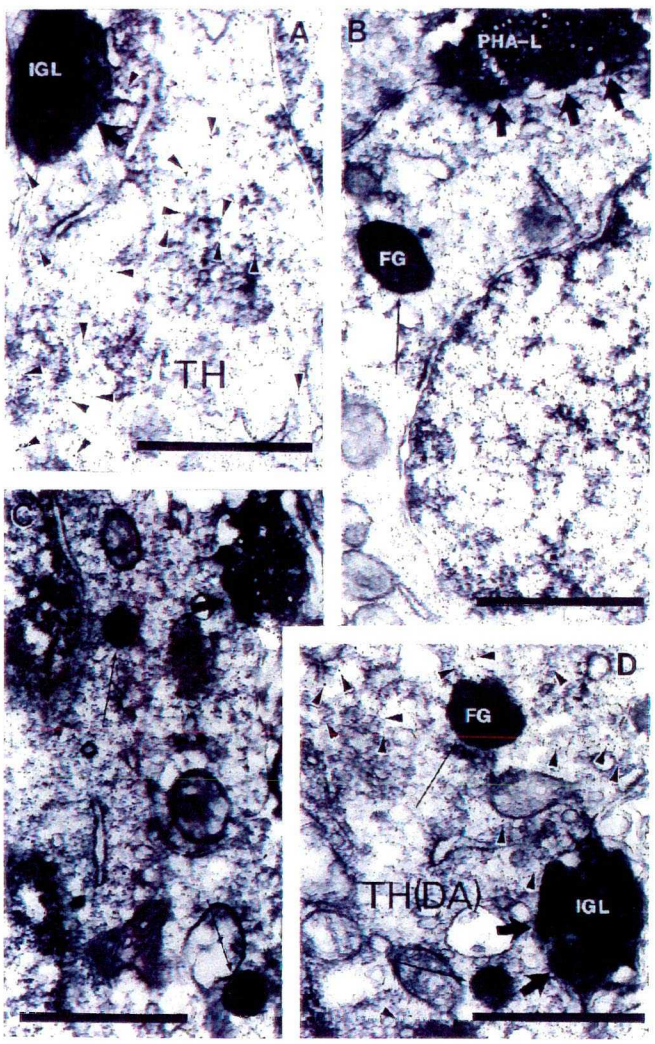

Fig. 7 Electron micrograph taken of the **ARC (A)**, **Pe (B)**, **MPO (C)** and the **AVPv (D)** from the material triple immunolabeled for **PHA-L**, **TH** (arrowheads on panels **A** and **D** point to immunogold) and FG (arrows). PHA-L-immunoreactive boutons originating in the **IGL** establish symmetric axo-somatic (**A-C**) and axo-dendritic (**D**) synaptic contacts (large arrows) with hypothalamic cells that contain TH and/or FG immunolabeling. Bar scales represent *1μm*.

PHA-L-TH double labeling

PHA-L immunoreactive fibers were seen in close apposition to TH-immunolabeled cells within the MPO, AVPv, periventricular and retrochiasmatic regions, dorsomedial nucleus and in an area between The arcuate nucleus and the ventromedial nucleus (Figs. 5 and 6 C&D). The IGL-target catecholaminergic cells were homogeneously distributed in the AVPv. In the periventricular region, most of these cells

were located in ventral areas, while in the subparaventricular zone most of these cells were concentrated in the bordering regions of the parvicellular paraventricular nucleus, dorsomedial nucleus and anterior hypothalamus. The majority of the appositions were between PHA-L-containing axons and the proximal dendrites of TH cells. However, axo-somatic connections could also be detected.

Triple labeled cells

In the hypothalamic regions (see above) where dopamine cells were detected to be retrogradely labeled, but most extensively in the AVPv, dark blue PHA-L boutons were found in contact with light brown TH-immunoreactive cell bodies and proximal dendrites containing retrogradely transported dark blue FG-immunopositive granules (Figs 5 and 6E-G2). Electron microscopic analysis revealed predominantly symmetrical synapses between PHA-L-immunoreactive boutons and neuroendocrine and/or dopamine producing cell bodies and dendrites (Fig. 7).

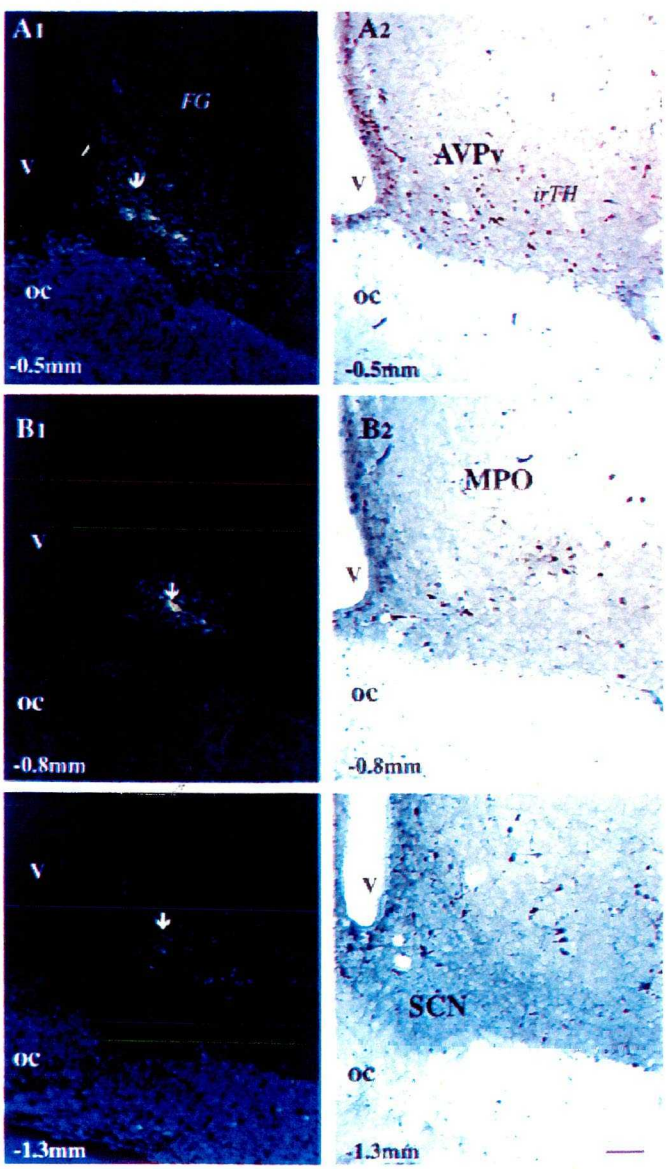

Fig. 8 A1-C2: FG injections in anterior hypothalamic sites. **A1, B1** and **C1: FG** injection sites (arrows) using ultraviolet light in the **AVPv (A1)**, **MPO (B1)** and an area above the **SCN (A3)**. **A2, B2** and **C2:** light micrographs of the areas corresponding to the FG injections immunostained for TH. The putative dopaminergic cells are present in the areas where FG was injected (compare **A1** with **A2**, **B1** with **B2**, and **C1** with **C2**). Bar scale represent 50 µm.

FG/enucleation experiments

Animals that were binocularly enucleated and received FG injections into hypothalamic sites were perfused 5 days after the parallel interventions.

This survival period was previously shown to be sufficient for the detection of anterogradely degenerated retinal axon terminals in the LGN (103) and to allow FG to travel a distance of 5-6 mm.

FG labeling

FG injection sites could be detected by fluorescence microscopy in discrete areas of the hypothalamus, including the anteroventral periventricular nucleus (Fig. 8A1) medial preoptic area (Fig. 8B1) and an area above the suprachiasmatic nucleus (Fig. 8C1). For this experiment, only those animals in which the FG injection avoided the SCN were used. Retrogradely labeled FG-immunoreactive perikarya and dendrites were observed throughout the hypothalamus. While almost all regions contained retrogradely labeled cells, the highest number of FG-accumulating neurons were found in the medial preoptic area, periventricular areas and the arcuate nucleus.

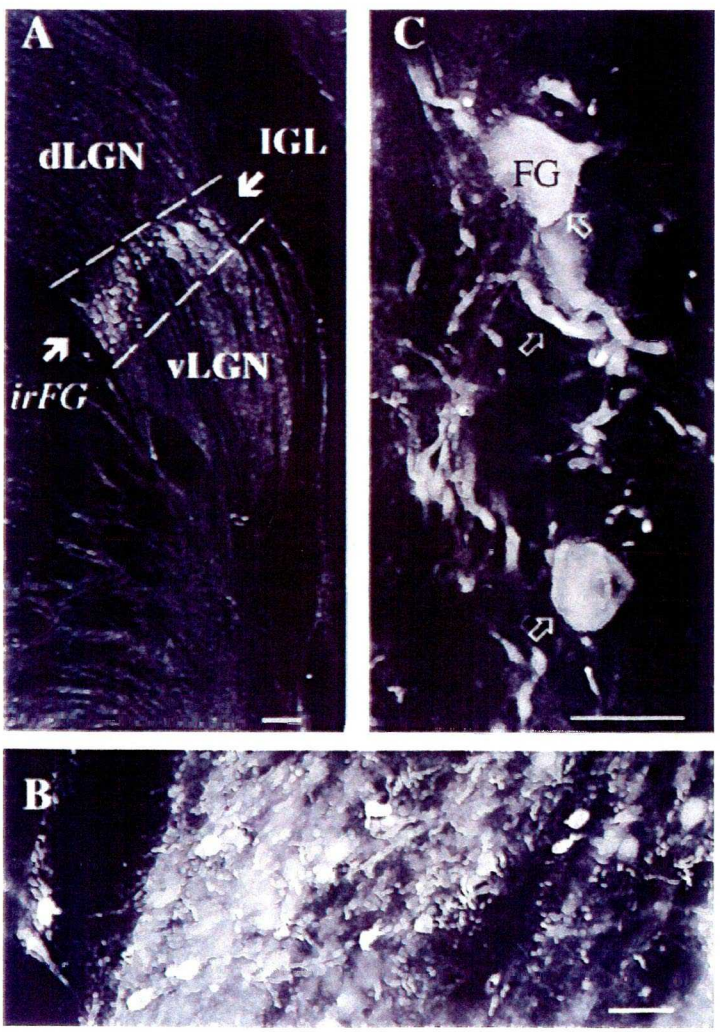

Fig. 9 A: light micrograph that demonstrates that retrogradely labeled, fluoro-gold immunoreactive (**irFG**) LGN cells are restricted to the **IGL** and are not present in the **dLGN** or **vLGN**. **B** and **C:** high power magnifications of FG-immunoreactive IGL cells. Arrows on Panel C point to **FG**-immunoreactive cells and dendrites within the IGL. Bar scales represent 100, 25 and 10 μm on panels **A, B** and **C**, respectively.

In the LGN, FG-immunoreactive perikarya were restricted to the IGL (Fig. 9). No retrogradely labeled neurons could be observed in either the vLGN or dLGN. Within the IGL, hypothalamo-projective neurons showed a homogeneous distribution (Fig. 9). While retrogradely labeled cells were present predominantly in the IGL ipsilateral to the injection site, numerous labeled perikarya could also be detected

in the contralateral IGL.

The immunoperoxidase labeling for FG was homogeneously distributed within the perikarya and dendrites of IGL neurons. Electron microscopic analysis revealed that all of the FG-immunoreactive perikarya of the IGL contained nuclei with numerous invaginations (Fig. 10A), whereas, nearby neurons with round nuclei (not infolded) never contained immunoperoxidase. While degenerated myelinated and unmyelinated axons and axon terminals were detected in the IGL, these fibers were never observed in close apposition to labeled or unlabeled cell bodies or proximal dendrites in the IGL. On the other hand, asymmetric synaptic contacts were frequently observed between degenerated retinal axon terminals and distal dendrites of both retrogradely labeled (Fig. 10B&C) and unlabeled IGL neurons

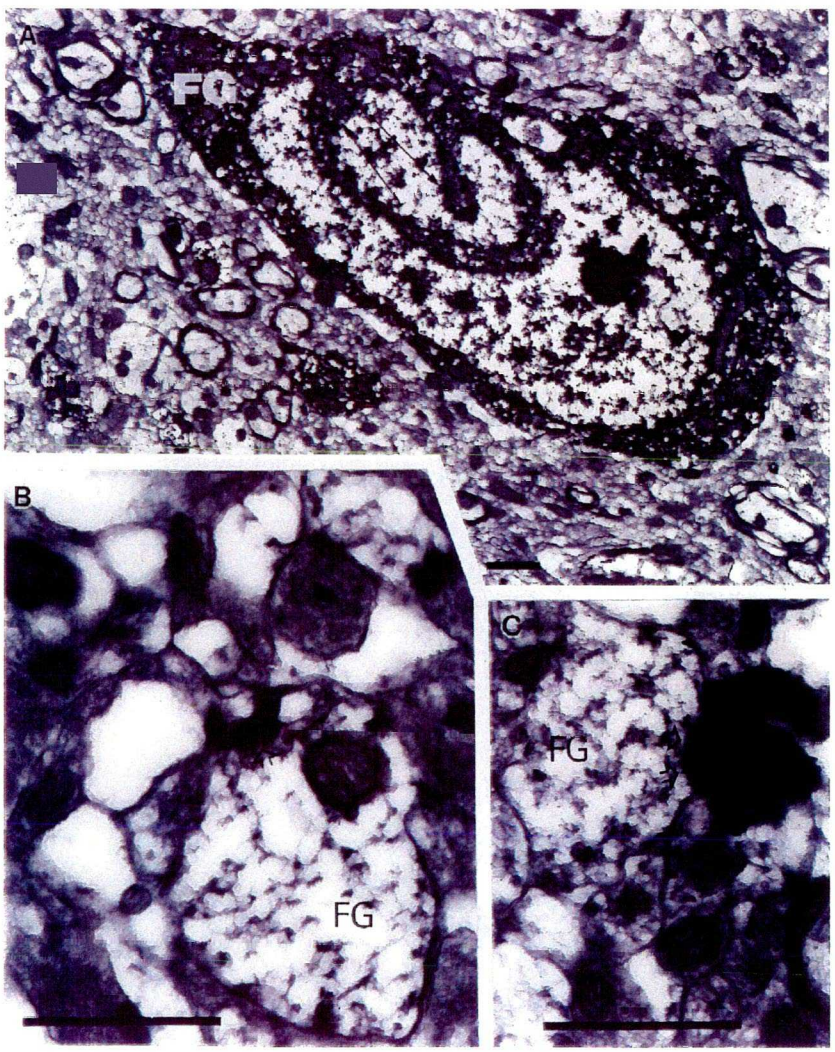

Fig. 10 Electron microscopic analysis of the IGL after hypothalamic FG injection and binocular enucleation. **A**: Ultrastructural analysis of a hypothalamus-projective (FG) IGL cell demonstrates that the nucleus contains several infoldings (arrows) and the immunolabeling for FG is homogeneously distributed in the cytoplasm. **B&C**: Asymmetrical synapses (open arrowheads) between degenerated retinal fibers and distal dendrites of IGL neurons containing immunoperoxidase for FG. Scale bars represent 1 μm.

OBJECTIVE 3 Can gonadal signals be integrated into the hypothalamo-pituitary axis outside of the hypothalamus, in the IGL?

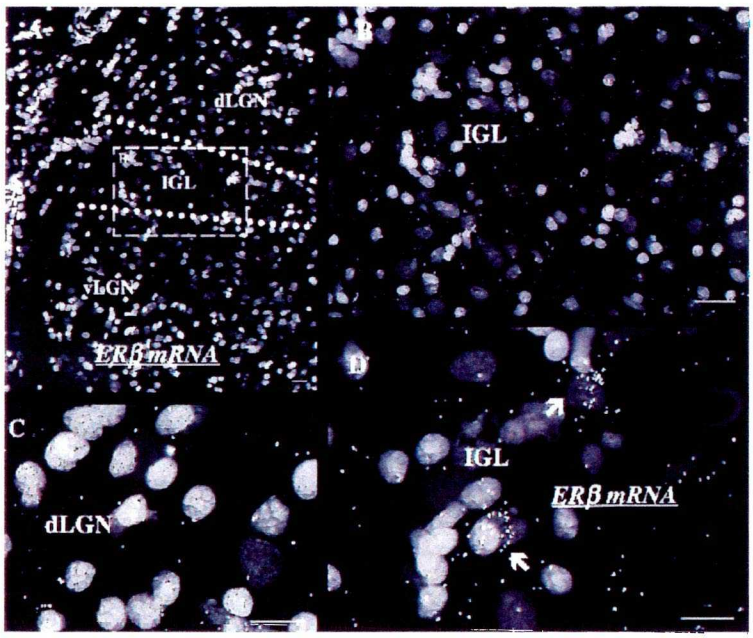

Fig. 11 *In situ* hybridization of ERβ mRNA in the lateral geniculated body. Silver grains are seen over hematoxylin-counterstained nuclei in the IGL and ventrale LGN.

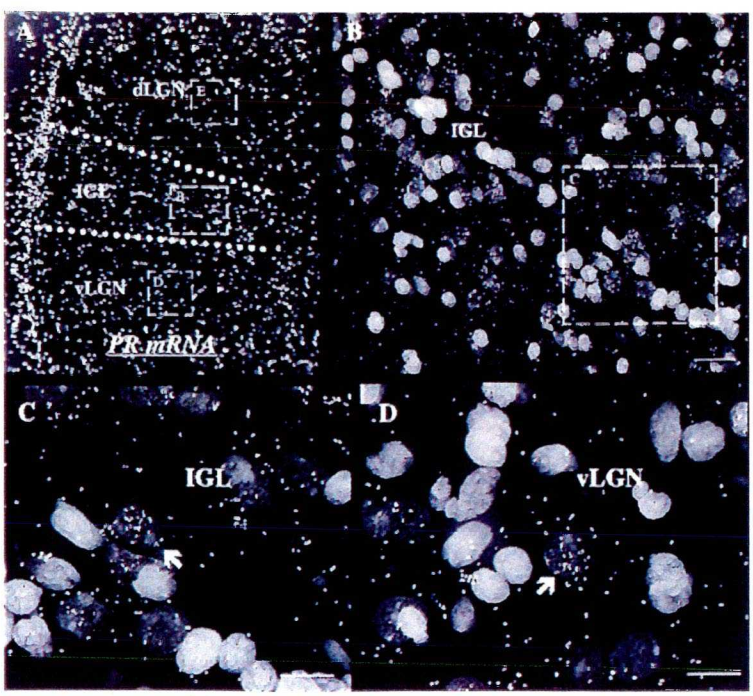

Fig. 12 *In situ* hybridization of PR mRNA in the lateral geniculated body. Silver grains are seen over hematoxylin-counterstained nuclei in the IGL and ventrale LGN.

ER-β mRNA

The regional distribution of ER-β mRNA-containing cells in the central nervous system have been described elsewhere (87). In this study, the focus is limited to the LGN, particularly the IGL. In accordance with a previous study, the density of silver grains over thalamic cells was much lower than that found in the limbic and hypothalamic sites. In fact, light microscopic analysis of the hybridized and counter stained section with low power magnification does not allow the appreciation of labeled cells in the LGN (Fig. 11A). However, high power magnification of different parts of the LGN revealed a relative abundance of cells having 5 times or higher number of silver grains than the same region over the ventricle representing the background level of labeling. Both in the vLGN and the IGL, labeled cells were homogeneously distributed (Fig. 11B and D), while in the dorsal LGN, no labeled cells were detected during this survey (Fig. 11C).

In the vLGN and IGL, approximately 10 % of cells expressed ER-β mRNA labeling.

PR mRNA

In the LGN, the distribution pattern of PR mRNA was similar to that of ER- β mRNA (Fig. 12): labeled cells were detected in the vLGN and IGL, but the dLGN lacked specific labeling for PR mRNA. These cells were homogeneously distributed in the vLGN and IGL, but were more abundant than ER- β mRNA containing cells. In these regions, approximately 25-30% of cells was found to be labeled for PR mRNA.

OBJECTIVE 4 Is the development of the biological clock under the control of gonadal steroids?

Aromatase immunolabeling

Immunoreactivity for aromatase was present in restricted regions of each major division of the telencephalon, metencephalon, and hindbrain, although, the differentiating cerebellum showed no immunoreactive cells. The distribution of immunopositive and unlabeled cells was identical for both antisera. Additionally, the appearance of aromatase immunoreactivity in perikarya of limbic and hypothalamic areas corresponded to earlier descriptions (89-93,104) and is detailed in another publication (90). While brains for both male and female animals were processed for aromatase immunoreactivity, comparison between staining intensity of males and females were not carried out. The pattern of aromatase immunoreactivity in different sensory regions of the rat brain is detailed below.

Olfactory system (Table 1)

We detected aromatase immunolabeling at all ages in the following olfactory areas: Cell bodies: ependyma and subependymal layer of the olfactory bulb, all divisions off the anterior olfactory nucleus, granule cell layer of the accessory bulb, lateral olfactory tract, piriform cortex. Axons and axon terminals. all of the aforementioned regions plus the accessory bulb, vomeronasal nerve, external and internal tubercle and internal granular and glomerular layers of the olfactory bulb. The appearance of immunolabeled processes increased from embryonic to postnatal age, although, the distribution pattern of cells and processes remained similar.

Visual system (Fig.13, Table 1)

Although no retinal ganglion cells were immunopositive, aromatase-immunoreactive axons were found in the optic tract by E14. Aromatase- positive fibers had not invaded central targets at this age, however, an increasing number of immunoreactive axon terminals were identified between E18 and P1 in the suprachiasmatic nucleus, lateral hypothalamus, lateral geniculate nuclei (dorsal, ventral divisions and most abundantly in the intergeniculate leaflet), the lateral posterior thalamic nucleus, and all layers of the superior colliculus. Although immunoreactive axon terminals were found in a diverse number of subcortical visual targets, aromatase-positive cell bodies appeared restricted to the superficial layers of the superior

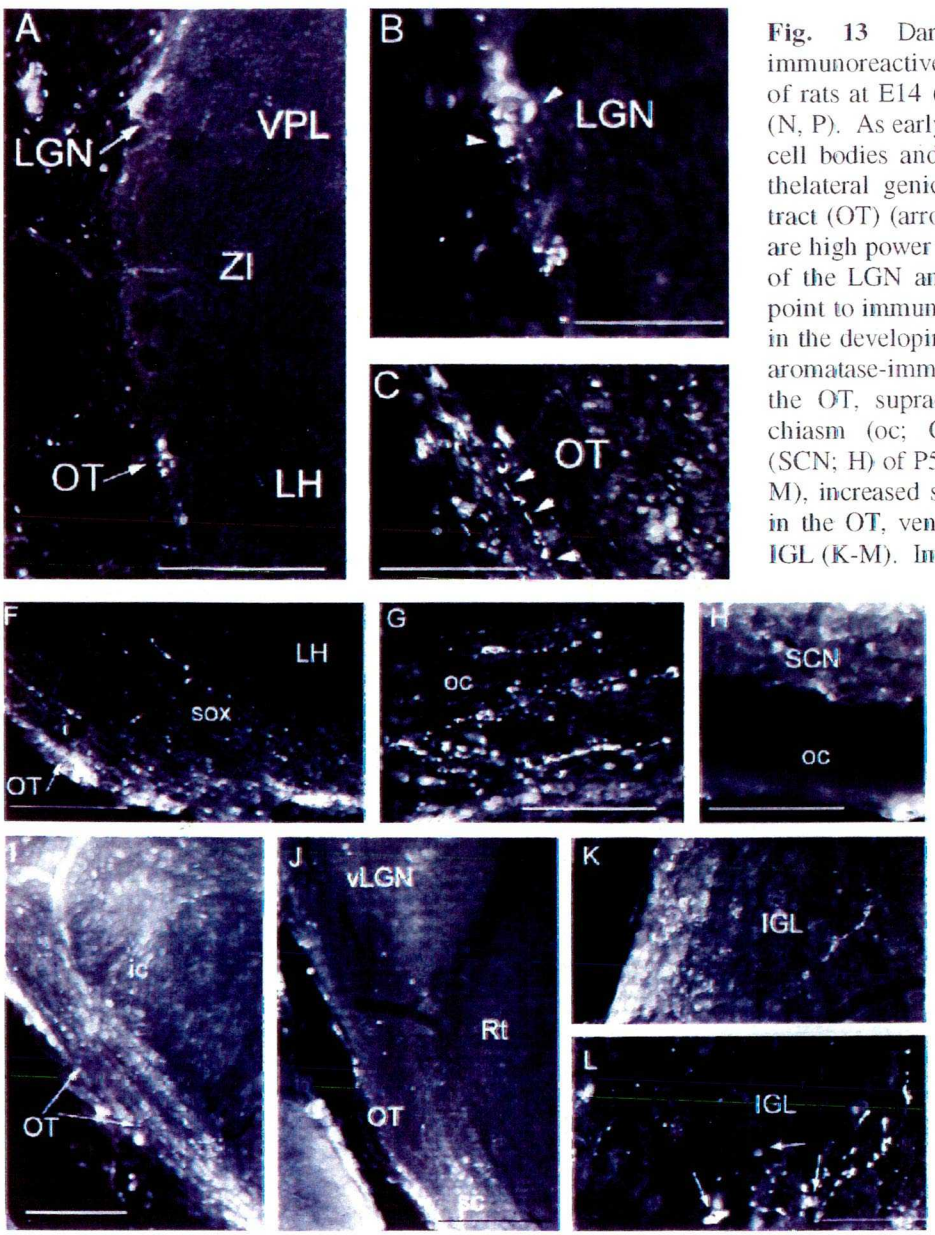

Fig. 13 Dark-field images of aromatase-immunoreactive cells in subcortical visual areas of rats at E14 (A-C), P5 (F-H), 10 (I-M) and 20 (N, P). As early as E14, aromatase was present in cell bodies and axons of visual areas, including thelateral geniculate nucleus (LGN) and optic tract (OT) (arrows on panel A). Panels B and C are high power magnifications of coronal sections of the LGN and OT, respectively. Arrowheads point to immunolabeled LGN cells (B) and axons in the developing optic tract (C). On panels F-H, aromatase-immunopositive profiles can be seen in the OT, supraoptic decussation (sox; F), optic chiasm (oc; G) and suprachiasmatic nucleus (SCN; H) of P5 animals. By postnatal day 10 (I-M), increased staining for aromatase can be seen in the OT, ventral LGN (I, J) and the emerging IGL (K-M). Immunolabeling for aromatase in cell bodies are present the intergeniculate leaflet (IGL) and the adjacent ventral LGN (vLGN; **L-M**). Panel **N** and **P** show aromatase immunolabeled neurons (arrows on panel **N**) in the superficial layer of the superior colliculus (sc) in animals at P20. VPL: ventral posterolateral thalamic nucleus; ZI: zona incerta; LH: lateral hypothalamus; Aq: mesencephalic aqueduct; ne: neuroepithelium; ic: internal capsule; Rt: thalamic reticulate nucleus. Bar scales represent 200 µm on panels **A, I-K**; 100 µm on panels **B, C, F-H, L-N**; and 10 µm on pane **P**.

colliculus and the intergeniculate leaflet.

Sensory areas in the hindbrain (Table 1)

Aromatase-immunoreactive fibers were detected in the caudal spinal trigeminal nerve, oral spinal trigeminal nucleus, spinal trigeminal tract, principle sensory trigeminal nucleus, peritrigeminal zone, mesencephalic trigeminal nucleus, glossopharingeal nerve, vestibulocochlear nerve, medial-, lateral-, and superior vestibular nuclei, nucleus solitary tract, olivocochlear bundle, all divisions of the lateral parabrachial nucleus, cuneate nucleus, and in the medial lemniscus. The densest immunolabeling was found in P10 and P20 animals.

Aromatase assay on the trigeminal tract, limbic and hypothalamic and cerebellar tissues:

In all four samples (limbic positive control, boiled limbic tissue for negative control, cerebellum for negative control, and sample from the spinotrigeminal tract), dpm counts were around 300 at 0 hour and was, therefore, considered as background. At 1 hour, cerebellar samples and the boiled limbic tissue showed unchanged dpm counts (300) while the limbic and the spinotrigeminal samples showed the

TABLE 1 Aromatase immunoreactivity in sensory areas of the developing rat brain

	Processes	*Cell bodies*
OLFACTORY SYSTEM		
Olfactory nerve layer (ON)	+++	
Internal plexiform layer of olfactory bulb (IPl)	++	
External plexiform layer of olfactory bulb (EPl)	++	
Glomerular layer of olfactory bulb (Gl)	++	
Mitral layer of the olfactory bulb (Mi)	+++	++
Inter granular layer of olfactory bulb (IGr)	+	+
Granule cell layer of accessory olfactory bulb (GrA)	++	+++
Accessory olfactory bulb (AOB)	++	
Anterior olfactory nucleus external (AOE)	+	++
Anterior olfactory nucleus medialis (AOM)	++	++
Anterior olfactory nucleus posterior (AOP)	+	+
Anterior olfactory nucleus lateralis (AOL)	+	+
Vomeronasal nerve (VN)	++	
Piriform cortex (Pir)	++	++
Medial orbital cortex (MO)	+++	++
VISUAL SYSTEM		
Optic tract	++	
Suprachiasmatic nucleus	++	++
Ventral lateral geniculate nucleus (VLG)	++	+
Intergeniculate leaflet (IGL)	+++	+++
Suprageniculate thalamic nucleus (SG)	++	
Nucleus optic tract (OT)	++	
Medial terminal nucleus of accessory optic tract (MT)	++	
Superficial gray layer of superior colliculus (SuG)	+++	++
Optic nerve layer of superior colliculus (Op)	++	
Intermediate gray layer of superior colliculus (InG)	+	
Intermediate white layer of superior colliculus (InWh)	+	
Deep gray layer of superior colliculus (DpG)	+	
Deep white layer of superior colliculus (DpWh)	+	
Zonal layer of superior colliculus (Zo)	++	++
AUDITORY SYSTEM		
Vestibulocochlear nerve (8n)	+++	
Superior vestibular nucleus (SuVe)	++	
Lateral vestibular nucleus (LVe)	++	
Medial vestibular nucleus ((MVe)	+	
Dorsal cochlear nucleus (DC)	++	
Lateral lemniscus (ll)	++	
External cortex of inferior colliculus (ECIC)	++	+
Medial geniculate body ventral (MGV)	++	
Medial geniculate body dorsal (MGD)	++	
Interstitial nucleus of mlf (IMLF)	++	
Olivocochlear bundle (ocb)	++	
Caudal interstitialis nucleus mlf (Cl)	+	
SOMATOSENSORY SYSTEMS		
Trigeminal nerve (5n)		
Spinal trigeminal tract (sp5)	++++	
Spinal trigeminal nucleus, oral (Sp5O)	+++	+++
Spinal trigeminal nerve, interpolar (Sp5I)	+++	+++
Spinal trigeminal nerve, caudal (Sp5C)	+++	+++
Peritrigeminal zone (P5)	++	
Principle sensory trigeminal nucleus ventrolateral (Pr5VL)	+++	++++
trigeminothalamic tract	++++	
Ventral posteromedial thalamic nucleus (VPM)	+++	
Mesencephalic trigeminal nucleus (Me5)	+++	++
Motor root trigeminal nerve (m5)	++	
Somatosensory pathways of the spinal cord		
Cuneate fasciculus	++	
Gracil fasciculus (gr)	++	
Cuneate nucleus (Cu)	++	
Gracil nucleus	++	
Medial lemniscus, medial part (ml)	++++	
Ventral posterolateral thalamic nucleus (VPL)	+	
OTHER SENSORY SYSTEMS		
Gustatory system		
Glossopharyngeal nerve (9n)	+++	
Nucleus solitary tract (Sol)	+++	
Medial parabrachial nucleus	+++	
Gustatory thalamic nucleus (Gu)	++	
Ventral posteromedial thalamic nucleus (VPM)	+++	
Viscerosensory systems		
Lateral parabrachial nucleus (LPB)		
Internal (LPBI)	++	
Dorsal (LPBD)	++	
Central (LPBC)	+++	
External (LPBE)	++	

conversion of 122±34 and 175±45 fmol [1 β -^{3}H] testosterone/mg protein, respectively. At 2 hour, negative controls showed no changes compared to the 0 and 1 hour values, and the conversion of [1 β -^{3}H] testosterone was 154±38 and 243±62 fmol/mg protein in the limbic and hindbrain tissues, respectively. At 4 hour, the 224±41 and 262±34 fmol of [1 β -^{3}H] testosterone was metabolized by the limbic and hindbrain tissues, respectively.

OBJECTIVE 5) Is the SCN input to GNRH cells gender specific?

This study provided light microscopic evidence for a sexual difference in the percentage of GnRH-synthesizing cells that receive VIP input. VIP-immunoreactive axons regularly showed interaction with GnRH neurons in both males and females (Fig. 14A and B). Yet, we found significantly more VIP-GnRH interaction in females (34.5 ± 4.1%) than in males (17.3 ± 2.1%; Fig 14C; $p<0.001$). Also, the frequency of VIP contacts on individual GnRH neurons was significantly higher in females (2.6 ± 0.23) as compared with males (1.3 ± 0.15; Fig 14D; $p<0.001$). The number of GnRH-immunoreactive neurons detected in the males (1254±185) and females (1423±232) showed no significant gender differences in accordance with previous results (105). Note that in the present study, the interaction between VIP

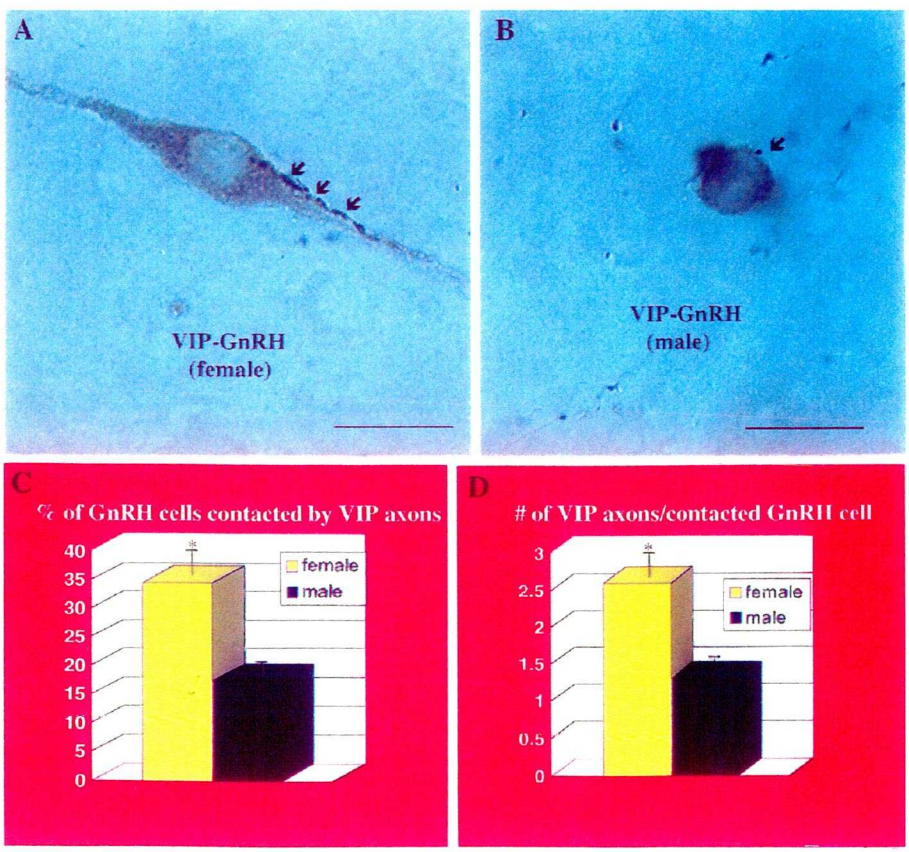

Fig. 14 **A** and **B**: Light micrographs showing typical interactions between VIP-containing fibers and GnRH-producing neurons in the medial preoptic area of female (**A**) and male (**B**) rats. Bar scales represent 10 μm. Panels **C** and **D**: Bar graphs illustrating (**C**) the percentage of GnRH neurons contacted by VIP-immunoreactive axons in females (yellow column) and males (blue column) and (**D**) the number of VIP boutons per GnRH that were contacted by VIP axons in females (yellow column) and males (blue column). * indicates $p<0.001$.

fibers and GnRH neurons was analyzed in females that were in metestrous. It was done to ensure that animals were exposed to similar gonadal steroid milieu. While the actual synaptic interaction between these systems may vary through the ovarian cycle due to fluctuating estradiol levels, the light microscopic appearance of this interaction does not seem to be different in animals with low estrogenic environment (present study) when compared to values taken from animals with gonadal steroid levels mimicking the preovulatory state (106). Since electron microscopic analysis was not conducted during this survey, further studies are needed to reveal whether the putative contacts between VIP axons and GnRH cells are synaptic and whether the number of these synaptic interactions vary during the estrous cycle. The sexual dimorphism in VIP-GnRH interaction that we report, however, corresponds to the studies of Chen et al. (107), who described that there is more synaptic apposition on GnRH neurons in females than in males. Thus, our data suggests that the gender specific synaptology of the rat GnRH neuronal system is due, at least in part, to VIP afferents to GnRH neurons.

DISCUSSION

1. The circadian clock, SCN, provides direct signals for neuroendocrine cells, including those producing GNRH and dopamine (Objective 1)

Methodology

Simultaneous application of the anterograde tracer PHA-L and systemic administration of the retrograde tracer FG was viable for demonstration of SCN inputs of neurons with direct access to blood vessels. The advantage of using FG instead of horseradish peroxidase (HRP), which labels neurons similarly to FG, is that that FG can stay for months within neurons (85,86), while HRP is eliminated within few days. The HRP-like appearance of FG enabled the use of the same chromogen (Ni-DAB) for PHA-L and FG immunoreactive profiles. Since the granular FG immunoreactivity was localized to lysosome-like organelles only (Fig. 3), it was possible to further immunolabel these cells for TH which antigen is located homogeneously in the cytoplasm. The use of dark Ni-DAB and light brown DAB reactions made it simple to distinguish between the three tissue antigens.

Intraperitoneal administration of FG results in retrograde labeling in neural cells that project to areas that lack blood brain barrier (85). These areas in the central nervous system include the so-called circumventricular organs i.e., the organum vasculosum laminae terminalis, subfornical organ, median eminence, and area postrema (108). In addition, the pineal gland and the posterior pituitary also lack blood-brain barrier (108). Therefore, the interpretation of the present observations without the results of previous anatomical studies delineating the contribution of different hypothalamic nuclei to the innervation of the aforementioned circumventricular organs, cannot be complete. For example, it is known that neurons in the medial septum-diagonal band-medial preoptic area region send projections to the organum vasculosum laminae terminalis, subfornical organ, and median eminence (for review see 108). On the other hand, the region of the mediobasal hypothalamus is considered to project predominantly to the median eminence and not to the other circumventricular organs (108).

SCN efferents to neuroendocrine- and/or TH-containing neurons

The present results show that a large number of hypothalamic sites are innervated by the SCN and, therefore, they are potentially the terminal field for relay of the circadian messages. Detailed description of the anterogradely labeled SCN efferents was not in the scope of this report, however, it can be concluded that the present results are in absolute agreement with the elaborated studies of Watts et al. (27,28). It has to be noted that the PHA-L injections were placed in the ventral aspects of the SCN, and only about 2% of SCN perikarya were labeled. Therefore, it could not be ruled out that other SCN cells may send processes to the median eminence. However, lack of FG-labeling in cells of the SCN after peripheral injection of this retrograde tracer, indicates that neurons in this area do not have direct access to vessels lacking the blood brain barrier. In light of the estimation that approximately 2% of SCN efferents were labeled in these experiments, the semiquantitative analysis on the connectivity between SCN efferents and neuroendocrine/non-neuroendocrine dopamine cells has to be interpreted with caution. *In vivo*, a higher incidence of interaction is expected.

In most of the hypothalamic nuclei where FG was observed, anterogradely-labeled SCN efferents were found to be in close apposition to FG-immunopositive cell bodies and dendrites. Previous pharmacological and morphological experiments demonstrated that hypothalamic neural systems which have a direct access to the portal vessels, and therefore, can be retrogradely labeled by peripheral FG injection, contain a variety of neuropeptides and neurotransmitters (for review see 109) including, GnRH (110,111), corticotropin releasing factor (CRF) (112), growth hormone-releasing hormone (GHRH) (113), thyrotropin releasing hormone (TRH) (114), somatostatin (115), dopamine (116), serotonin (117, 118) galanin (86) and gamma amino butyric acid (GABA) (119, 120). Our present observations of SCN efferents on neuroendocrine cells suggest that at least some of these systems may be directly regulated by the SCN. In accordance, recent studies indicated that GnRH neurons are indeed targets of axon terminals originating in the SCN (95,96,121).

The triple immunolabeling experiments of the present study revealed that SCN-target, retrogradely labeled cells in different hypothalamic sites express TH immunoreactivity. TH-immunoreactive cell bodies in the hypothalamus represent exclusively dopaminergic neurons,

since immunostaining for the enzymes responsible for norepinephrine or epinephrine synthesis have failed to reveal immunoreactive perikarya in the hypothalamus (97,122,123). Therefore, the present results provide morphological basis for the information flow between the SCN and dopamine cells. A population of these dopaminergic neurons was retrogradely labeled indicating that they contact portal capillaries either in the external layer of the median eminence or in the portal capillaries of the posterior and intermediate lobe of the pituitary. In either case, dopamine released into portal vessels can influence lactotrophs in the anterior pituitary as well as the release of other hypophysyctropic hormones such as GnRH. On the other hand, dopamine neurons, which lacked retrogradely transported FG, were also found to be targets of SCN efferents. These cells are known to innervate wide variety of regions in the central nervous system (48,97). For example, most of the hypophysiotropic hormone-producing neural systems, including GnRH (124), are targets of considerable amount of TH-containing axon terminals. Thus, the current findings suggest that SCN signals may reach hypophysiotropic hormone-producing neural systems indirectly as well, via dopamine interneurons.

Functional implications

The present results provided morphological basis for the information flow between the circadian pacemaker suprachiasmatic nucleus and neuroendocrine neurons. The majority of SCN targets retrogradely labeled neurons were found in the medial preoptic area, periventricular area and in the lateral aspects of the arcuate nucleus. The vast majority of these neurons send their projections to the median eminence, while a portion of cells in the medial preoptic area may have been labeled from the organum vasculosum laminae terminalis (96). While there is a paucity of information on the function of the OVLT, the role of the median eminence and its portal vessel system in the regulation of anterior pituitary functions is well-established (32).

Neurons with direct access to portal veins contain different neurotransmitters and modulators, as well as specific trophic and static hormones which released from the nerve terminals to the portal capillaries, reach the anterior pituitary and alter the production and secretion of pituitary hormones. Secretion of most of the anterior pituitary hormones including gonadotrophins and prolactin show diurnal variations (34-36,58,65,125-128). Under normal physiological conditions, the entrainement of these rhythms is by the light dark cycle (127). The

light dark cycle influences the neuroendocrine hypothalamus, at least in part, through direct retinal projections to the SCN (22,127).

Prolactin secretion

Production and secretion of prolactin show diurnal patterns and are under the control of the mediobasal hypothalamus. Dopamine secreted into the portal capillaries is considered to be the major regulatory substance in prolactin production and release (5, 129). On the day of proestrus, and at every day in estrogen-primed ovariectomized rats, prolactin secretion from the anterior pituitary is increased in the afternoon (130). This elevation of prolactin is , at least in part, due to decreased dopamine release induced by the preovulatory estrogen surge (131). It was demonstrated that in ovariectomized, estrogen-primed rats, significant decreases of median eminence dihidroxyphenilacetic acid (DOPAC) and dehydroxyphenylalanine (DOPA) occur in parallel with the increased prolactin secretion (132). The nature of these events is circadian (42), and, destruction of the suprachiasmatic nucleus abolishes the development of afternoon prolactin surges (37,132). The present study demonstrating direct connection between the SCN and neuroendocrine dopamine cells offers a neural pathway via circadian signals alter prolactin secretion.

Gonadotropin secretion

Circadian activity is also characteristic for both the daily release and the preovulatory release of gonadotrophins (127). It is suggested that the release from the inhibitory tone on GnRH neurons initiates both the afternoon and preovulatory gonadotrophin surges. Our finding of a direct synaptic interaction between SCN efferents and GnRH neurons provide a signaling modality for circadian regulation of GnRH neurons. On the other hand, since a populations of dopamine neurons in the periventricular areas were shown to project to the preoptic area and terminate on GnRH neurons (124), the innervation of non-retrogradely labeled TH cells in the same regions by SCN efferents raise the possibility that suprachiasmatic signals may reach GnRH cell bodies via these catecholamine neurons. Furthermore, neuroendocrine dopamine cells too may convey circadian signals to GnRH cells at the level of the median eminence. It is reasonable to postulate that since the SCN efferents are most probably inhibitory in nature (vasoactive intestinal polypeptide- and GABA content [133,134]), the activation of SCN neurons

may inhibit the dopamine neuronal network resulting in a disinhibition on GnRH neurons at the level of either the cell bodies (preoptic area) or axon terminals (median eminence).

This study using anterograde and retrograde tracing techniques in combination with immunocytochemistry, provided evidence that: 1) the circadian pacemaker suprachiasmatic nucleus send direct efferents onto neuroendocrine cells of different hypothalamic nuclei, 2) a subpopulation of SCN target neuroendocrine cells contains dopamine and GnRH, and 3) suprachiasmatic efferents do not reach fenestrated capillaries. These observations suggest that the circadian pacemaker has no direct effect on the regulation of anterior pituitary functions, but, indicate a pathway via circadian signals are integrated into the hypothalamo-pituitary-gonadal axis. It needs to be explored whether the integration of hormonal and circadian signals, a mandatory process in the regulation of anterior pituitary, which was indicated to occur in populations of hypothalamic neurons (135) may be the same cells that were found to be neuroendocrine in the present study.

2. The IGL in the lateral geniculate body can provide signals to neuroendocrine cells independent of the SCN (Objective 2)

LGN efferents innervated various hypothalamic sites. While an abundant network of LGN fibers was detected in the SCN, a comparable innervation of the subparaventricular zone and other periventricular structures was also observed (Fig. 2). These results are in agreement with previous demonstrations of LGN efferents in various regions of the hypothalamus (29,53-55,136). However, with the exception of a recent preliminary report (55), this study is the first to provide a detailed description of LGN efferents throughout the entire rat hypothalamus and to demonstrate an almost complete overlap between SCN and IGL projections in different hypothalamic nuclei.

The exclusive appearance of retrogradely labeled cells in the IGL following hypothalamic FG injections is also in accordance with the result of Moore et al. (55). In anterograde tracing experiments, they found that the IGL and not the vLGN contributes to the innervation of the hypothalamus. Our electron microscopic analysis revealed that the retrogradely labeled IGL perikarya contained exclusively infolded nuclei and IGL projections

established symmetric synaptic contacts with hypothalamic target cells. These characteristics are associated with inhibitory neurons (137). Previous immunocytochemical studies demonstrated that IGL neurons produce enkephalin, neuropeptide Y and GABA (138,139). It was also shown that IGL neurons and their projections to the SCN colocalize NPY and GABA (140,141) and that these peptidergic terminals, in part, established symmetric synaptic contacts (22). Thus, it is likely that the geniculohypothalamic tract innervating extrasuprachiasmatic sites may also be a GABAergic, NPY-containing pathway.

These experiments revealed that a population of LGN-targeted neurons in the hypothalamus are neuroendocrine cells, i.e., they have direct access to the portal vasculature of the median eminence or the organum vasculosum laminae terminalis. These cells, including those producing dopamine, were most frequently found in periventricular areas. The same hypothalamic cell populations were previously found to receive SCN input (101), raising the possibility of convergent SCN and IGL inputs on the same hypothalamic perikarya. In light of the fact that the parent cells of the IGL efferents were found to receive direct visual input, it is reasonable to suggest that the integration of visual and circadian signals into the hypothalamo-pituitary axis may occur on the final output neurons of the hypothalamus adding another level of redundancy to the pathways via which the environment may regulate hormone secretions.

An increasing body of data indicate that visual signals may be conveyed to hypothalamic sites by pathways other than the SCN. In addition to direct retinal input to different hypothalamic sites (24,25,142-146), the present and previous studies (53,54,147) found that there is an extensive projection of IGL neurons to hypothalamic sites, including the medial septum, diagonal band of Broca, bed nucleus of the stria terminalis, MPO, AVPv, periventricular areas, subparaventricular zone, dorsomedial nucleus and a cell-sparse zone between the arcuate nucleus and the ventromedial hypothalamic nucleus. It was also demonstrated that retinorecipient IGL neurons innervated neuroendocrine cells, including those producing dopamine. These observations indicate that the participation of the IGL in the regulation of central mechanisms may not be restricted to the alteration of SCN activity, but the IGL may directly convey photic stimuli to neuroendocrine cells.

Functional considerations

Production and secretion of prolactin and LH from the anterior pituitary show diurnal patterns and are under the control of the mediobasal hypothalamus. Dopamine secreted into the portal capillaries is considered to be the major regulatory substance in prolactin production and release (33,129). On the day of proestrus and every day in estrogen-primed ovariectomized females, prolactin and LH secretions from the anterior pituitary increase in the afternoon (130). This elevation of prolactin is , at least in part, due to decreased dopamine release (131). Significant decreases of median eminence dihidroxyphenilacetic acid (DOPAC) and dehydroxyphenylalanine (DOPA) also occur in parallel with the increased prolactin secretion (132). Regarding LH secretion, it is suggested that the release from the inhibitory tone on GNRH neurons initiates both the afternoon (36) and preovulatory gonadotropin surges.

The SCN constitutes an essential component for normal control of LH and prolactin secretion in rodents. Destruction of the circadian clock blocks the preovulatory LH and prolactin surges and induces persistent estrus accompanied by hyperprolactinemia in intact female rats (132). A similar outcome occurs during constant light exposure which first induces a delay (45), but then abolishes the daily and preovulatory gonadotropin and prolactin surges (38,39,46). Interestingly, under these conditions, the circadian SCN activity will free run (54). A plausible cause for altered hormone secretions could be that the rhythm of the free running circadian pacemaker during constant light eventually will split into two running cycles (148-152). This, in turn, will impair most circadian rhythms and also underlies split daily surges of LH (151,152). Since these changes in circadian function were not described in rats, it is likely that during constant light exposure, there is a continuous signal from the eye to the final output neurons of the hypothalamus that maintains a subtle, but, steady activation of anterior pituitary cells producing LH and prolactin.

Our results elucidate a pathway through which these continuous signals can be conveyed from the eye to hypothalamic cells via the IGL. The observation that exposure to constant light induces the continuous expression of the early proto-oncogen, c-fos, in IGL cells but not in SCN neurons (153,154) raises the possibility that the neuroendocrine cells described to receive IGL

(present study) and SCN (101) inputs may be continuously altered by IGL rather than SCN signals. To further elucidate the interaction of SCN and IGL signals in the regulation of these hypothalamic cells exposed to constant light, the localization and possible segregation of these inputs on the same hypothalamic perikarya need to be determined.

Of particular interest regarding prolactin and LH secretions, are those IGL-targeted dopamine cells that are located in the anteroventral periventricular nucleus. The critical role of this extrasuprachiasmatic area in the rhythmic regulation of anterior pituitary hormones has been recognized: similar to the effects of constant light exposure, it was found that selective destruction of this area abolishes ovarian cycles and results in the emergence of constant vaginal estrus (128). Therefore, it is likely that the IGL input to neuroendocrine and non-neuroendocrine dopamine cells of the AVPv may significantly contribute to the development of altered anterior pituitary hormone secretion induced by constant light exposure. *Prolactin secretion:* neuroendocrine dopamine cells of the AVPv and arcuate nucleus are known to send efferents to the median eminence region (47,49) to participate in the suppression of prolactin secretion (33). Since the excitatory visual input on IGL neurons may be translated to an increased inhibitory tone on the neuroendocrine dopamine cells (putative inhibitory projections from the IGL), the consequent decreased dopamine secretion can underlie a steady elevation of prolactin secretion during constant light. *Gonadotropin secretion:* Dopamine interneurons of the AVPv were found to innervate GnRH cells (124) and to receive IGL efferents (present study). Therefore, an increased inhibitory input (from the IGL) on these dopamine cells induced by constant light may affect the activity of GnRH neurons leading to a continuous, steady trigger for LH secretion.

In conclusion, this study provides evidence for a monosynaptic pathway between IGL neurons and hypothalamic cells outside the SCN. It was demonstrated that IGL efferents innervate neuroendocrine cells, including those producing dopamine, and that their parent cells received direct retinal input. Therefore, it is suggested that a signaling modality exists between the eye and hypothalamic cells not involving the SCN that can regulate neuroendocrine and autonomic functions.

3. Gonadal signals can be integrated into the hypothalamo-pituitary axis outside of the hypothalamus, in the IGL (Objective 3)

This study provided evidence for the expression of ER-β and PR mRNA in the ventral LGN and IGL using in situ hybridization hystochemistry. The riboprobes used in the present study have been well characterized and shown to be specific for the transcripts these gonadal steroid receptor genes (87).

The amount of ER-β and PR transcripts present in vLGN and IGL cells seemed to be lower compared to other limbic and hypothalamic regions where the abundance of silver grains over cells was observed to be much higher. A comparative analysis of mRNA labeling intensity within the rat brain has been reported for ER-β. In that study, while the presence of ER-β mRNA has been mentioned in the vLGN, the IGL was not analyzed separately and no quantitation was given in regard to the size of the neuronal population within this thalamic region expressing ER-β mRNA.

The existence of ER-β and PR transcripts in the vLGN and IGL further underlines the suggested importance of the IGL in the regulation of the hypothalamo-pituitary axis. This finding together with the results of Objective 2 inspire us to speculate that hormonal signals may get integrated into the hypothalamo-pituitary axis outside of hypothalamic and limbic regions. In particular, we propose that estrogen and progesterone regulate the light input to neuroendocrine cells at the level of the IGL in the lateral geniculate body.

4. The development of the biological clock is under the control of gonadal steroids (Objective 4)

This study clearly demonstrated that both components of the extended biological clock, the SCN and IGL, are sites of local estrogen production during the critical developmental period. This observation raises the possibility that sexual dimorphisms in the extended biological clock may exist and support the gender specific regulation of anterior pituitary hormones. Part of this

hypothesis was tested in Objective 5, when the SCN-derived VIP innervation of GnRH neurons was assessed in male and female rats.

Aromatase in other sensory areas of the rat brain

In addition to providing evidence for local estrogen formation in the biological clock, the aromatase immunolabeling of developing brain regions yielded some striking new observations. Although these results may not directly relate to the scope of this thesis, since it was acquired during this project, a short discussion of them may be worthwhile.

Since the discovery of estrogen formation by aromatase in the embryonic and early postnatal central nervous system (155), extensive research has been conducted to decipher the significance of locally formed estradiol in brain development. These studies demonstrate that testosterone-derived estrogen is a key player in the emergence of sex differences in limbic/hypothalamic morphology and related functions (68,70,156,157). Biochemical approaches revealed that estrogen is synthesized in limbic and hypothalamic regions (73,75,155,158,159). However, the complex afferent and efferent connections of these regions mandated the examination of the cellular localization of aromatase to understand which neural networks underlie estrogen- induced changes in neural function during a restricted developmental critical period. Although progress has been made to identify these aromatase containing neuronal populations using different antisera generated against the aromatase peptide (91-93,104,160-163) or its fragments (89,90), the possibility that aromatase may also be present in extrahypothalamic and extralimbic areas has not been adequately explored.

Our present observations using two aromatase antisera with different immunological characteristics demonstrate the presence of aromatase immunoreactivity in cell bodies and axonal processes of sensory areas in the developing rat brain. Both antiserum labeled previously identified neuronal populations in the amygdala, bed nucleus of the stria terminalis, lateral septum, medial preoptic area and ventromedial nucleus (92,93,104,160-163). In situ hybridization studies also demonstrated that the same neuronal populations also express aromatase mRNA (164,165). The antiserum that was generated against the synthetic polypeptide labeled the entire axonal processes of limbic and hypothalamic neurons revealing the projection

field of aromatase-containing neuron populations (90). The antiserum that was generated against the entire enzyme also recognizes axonal processes but to a lesser extent (93). Axonal aromatase was also reported in the synaptosomal fractions of the quail brain (166). In addition, the specificity of the antisera was confirmed by radioimmunassay for testosterone metabolism in different limbic and sensory tissues.

The present finding of the selective expression of aromatase activity restricted to specific cellular compartments of sensory regions of the CNS may explain why previous biochemical studies failed to reveal aromatase activity in non-limbic regions of the rat brain. We assume that the presence of aromatase activity in these regions was missed since these studies could not identify and biopsy the restricted aromatase-positive brain regions identified by our immunocytochemical analysis. The mapping of aromatase-immunoreactivity in the present study enables us to target specific regions of the embryonic and postnatal rat brain for future biochemical analyses. It should be noted that a recent study demonstrated aromatase activity in hindbrain explants taken from perinatal animals (167).

The visualization of axonal aromatase may allow for the elucidation of signaling pathways and connected functions directly influenced by locally formed estradiol during development. Estrogen-regulated sex specificity is due to the sexual dimorphic availability of the substrate androgen that is present at a higher concentration in male fetuses (168,169). The presence of aromatase and aromatase activity in developing sensory processes points to the possible importance of estrogen in the maturation of these networks. Locally formed estradiol regulates apoptosis (170), process formation and growth (171), as well as the formation of synapses (172) in the developing CNS. In the limbic system and hypothalamus, estrogen plays a crucial role in the sex specific development of morphology and function (70,156,157). Therefore, it is reasonable to suggest that locally formed estradiol may participate in the development of olfactory, visual, auditory, gustatory and somatosensory pathways.

Recent evidence has identified sexual dimorphisms in rat sensory areas. For example, sex differences were detected in the accessory olfactory system (173), as well as in certain parts of the visual system (174) of the rat and the teleost fish (175). Our data may provide the

underlying mechanism for the emergence of these sexual dimorphisms and indicate that other sensory systems may also develop under the control of locally formed estradiol. We propose that the emergence of sex differences in different sensory systems occurs through the aromatase-mediated conversion of testosterone to estradiol.

One characteristic of aromatase-containing cells and their processes is that these cellular elements may not only capable of influencing themselves, but could exert paracrine effects (176) on neighboring structures. The diffusion of estrogen from aromatase-positive cells in sensory regions may have important implications for the developing CNS. For example, the spinotrigeminal tract, found to contain the high amounts of aromatase activity, courses through almost the entire length of the developing hindbrain. Estrogen production associated with this tract may influence the maturation of structures surrounding this area of the brainstem, including those regions that do not display aromatase activity. Similarly, the ventral lateral geniculate body and the intergeniculate leaflet of the geniculate body may have the capacity to provide sufficient amounts of estradiol for developing neurons of dorsal areas of the lateral geniculate nucleus.

Our present results raise the question of what mechanism may mediate estrogenic action in these sensory sites. While it is thought that nuclear estrogen receptors mediate most of the actions of estradiol, it has becoming evident that non-classical receptor mediated mechanisms also participate in these processes. In accordance with this heterogeneity in estrogenic actions, some areas where sensory processes and cells were found to contain aromatase, different estrogen receptor subtypes (alpha and beta) are abundant during that developmental period and adulthood, for example, in the suprachiasmatic nucleus, intergeniculate leaflet and the primary sensory nucleus of the trigeminal nerve (87,177,178). It remains to be determined which combination of steroid hormone receptors and other second messenger systems mediate the action of estrogen in developing sensory regions of the brain.

5. The SCN input to GnRH cells is gender specific (Objective 5)

The VIP input of the medial septum-diagonal band-medial preoptic area region, the site where most of the GnRH neurons are located (105), may derive from different forebrain and

hypothalamic regions. However, recently we demonstrated that the vast majority of the VIP containing afferents of GnRH neurons in the preoptic region is derived from the SCN (106). Following bilateral destruction of the SCN, approximately 80% of the VIP contacts on GnRH neurons of female rats were lost (95). Consequently, the 4-fold higher frequency of interaction between VIP boutons and GnRH neurons in females may be due to gender specific projections from the SCN to these neurons. This suggestion is supported by our recent observation showing the presence of estrogen synthetase (aromatase) in cells and processes of the SCN between embryonic day 14 and postnatal day 20 (90). This is a critical perinatal period during which aromatized androgen derived from the testes exerts its organizational effect on the central nervous system leading to the emergence of sexual dimorphisms (179,180). Indeed, females treated with androgens neonatally fail to display regular cycles during adulthood and do not show a LH surge following steroid treatment (181). On the other hand, the possibility that gonadal steroids exert an effect one VIP production in the adult animal cannot be excluded. For example, the VIP content of the hypothalamus was found to be higher in adult cycling females than in intact males (182), and gonadectomy reduced hypothalamic VIP mRNA in females but not in males (183). Also, an immunocytochemical study in the jerboa, a seasonal breeder, indicated sexual differences in VIP content of the SCN associated with sexual activity (184). Therefore, it is likely that the emergence of gender-specific VIP input of the rat GnRH neural system is regulated by developmental mechanisms as well as by the effects of gonadal steroids during adult life.

The role of VIP in the regulation of GnRH and LH release is ill-defined. Contradictory data exists showing that VIP can stimulate the steroid induced LH surge under certain experimental conditions (185), while it inhibits gonadotrophin release when administered under other conditions (186,187). Yet, the critical role of the SCN, which is likely to be the source of the VIP input to GnRH neurons, has been established for both the diurnal and the preovulatory surge of gonadotrophins (35,36,58,188). Moreover, we have found a preferential activation of those GnRH neurons that show interaction with VIP-containing fibers, especially around the onset of the LH surge (106). This suggests that VIP-input on GnRH neurons is involved in the regulation of the LH surge.

In conclusion, the present study provides anatomical evidence for a sexual difference in the input of VIP fibers on the GnRH neuronal system in the rat. The VIP-input on GnRH neurons

Given these data, we suggest that such a sexual difference provides a morphological basis for the observed sexual dimorphism in the regulation of gonadotrophin release between male and female rats.

6. Synopsis

The circadian/visual system is a phylogenetically preserved system that allows for the temporal organization of the environment and the organism. In this thesis we carried our experiments that provide new insights into a particular output of the extended biological clock, i.e., the rhythmic regulation of the hypothalamo-pituitary axis (Fig. 15). We demonstrated alternate routs of signaling from the circadian clock, SCN, and eye to the neuroendocrine hypothalamus. We also revealed that the mandatory integration of hormone signals into the hypothalamo-pituitary axis could occur outside of the hypothalamus and limbic system, in the intergeniculate leaflet of the lateral geniculate body. These signaling pathways together with the demonstration of gender specific SCN input to neuroendocrine cells and local estrogen formation in the extended biological clock during the critical developmental period lead us to conclude that the female-specific emergence of circadian gonadotropin secretion is supported by sexual dimorphisms in the biological clock. Further studies are needed to test this proposition and the functional significance of our results.

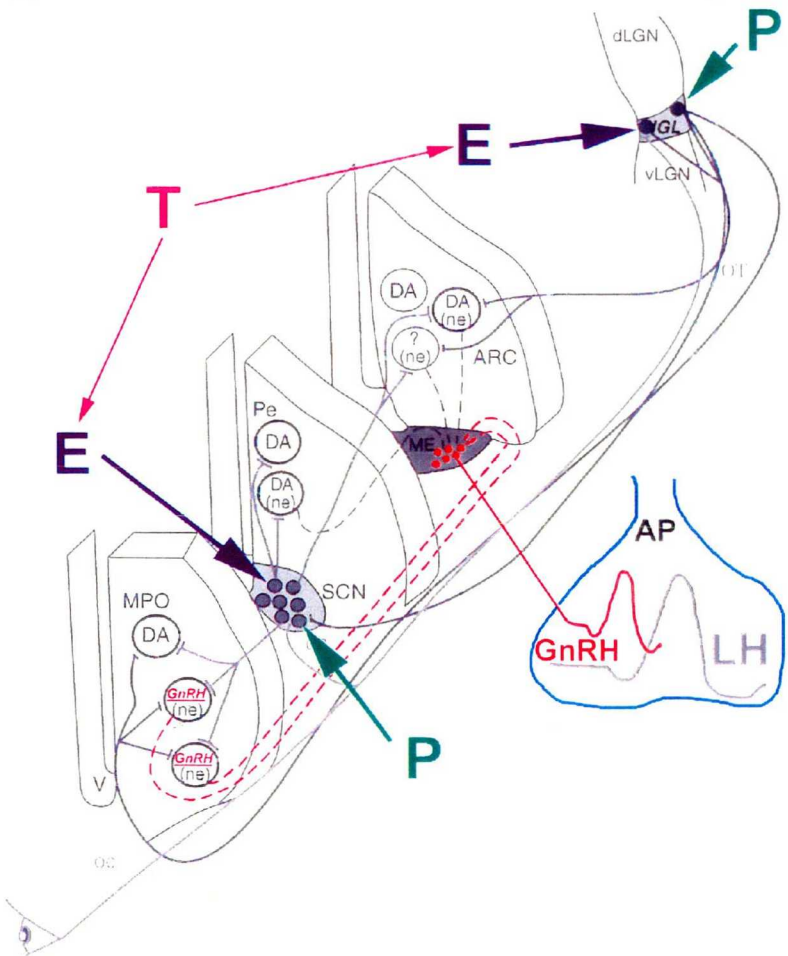

Fig. 15 Schematic illustration of the results gathered during these experiments providing a morphological substrate for the relationship between hormone signals, visual, circadian and neuroendocrine cells in the hypothalamus.

proposition and the functional significance of our results.

REFERENCES

1. Albright DL, Voda AM, Smolensky MH, HIS B, Decker M 1989 Circadian rhythms in hot flashes in natural and surgically-induced menopause. Chronobiology International 6:279-284.
2. Baker ER, Best RG, Manfredi RL, Demers LM, Wolf GC 1995 Efficacy of progesterone vaginal suppositories in alleviation of nervous symptoms in patients with premenstrual syndrome. J Assist Reprod Genet 12:205-209.
3. Brace M, McCauley E 1997 Oestrogens and psychological well-being. Annals of Medicine 29:283-290.
4. Buchholz NP, Mattarelli G, Buchholz MM 1994 Post-orchidectomy hot flushes. European Urology 26:120-122.
5. Carranza-Lira S, Murillo-Uribe A, Marinez Trejo N, Santos-Gonzales J 1997 Changes in symptomatology, hormones, lipids, and bone density after hysterectomy. Int J Fertil Womens med 42:43-47.
6. Clark AJ, Flowers J, Boots L, Shettar S 1995 Sleep disturbance in mid-life women. J Adv Nurs 22:562-568.
7. Guthrie JR, Dennerstein L, Hopper JL, Burger HG 1996 Hot flushes, menstrual status, and hormone levels in a population-based sample of midlife women. Obstetrics and Gynecology 88:437-442.
8. Halbreich U 1997 Role of estrogen in postmenopausal depression. Neurology 48:S16-19.
9. Hendrick V, Alshuler LL, Burt VK 1996 Course of psychiatric disorders across the menstrual cycle. Harvard Review of Psychiatry 4:200-207.
10. Huerta R, Mena A, malacara JM, de Leon JD 1995 Symptoms at the menopausal and premenopausal years: their relationship with insulin, glucose, cortisol, FSH, prolactin, obesity and attitudes towards sexuality. Psychoneuroendocrinology 20:851-864.
11. Malacara JM, Huerta R, Rivera B, Esparza S, Fajardo ME 1997 Menopause in normal and uncomplicated NIDDM women: physical and emotional symptoms and hormone profile. Maturitas 28:35-45.

12. McReynolds SM, Freidberg SR, Guay AT, Lee AK, Pazianos AG, Hussain SF 1995 Hot flushes in man with pituitary adenoma. Surgical Neurology 44:14-17.
13. Pariser SF, Nasrallah HA, Gardner DK 1997 Postpartum mood disorders: clinical perspectives. J Womens Health 6:421-434.
14. Pearlstein T, Rosen K, Stone AB 1997 Mood disorders and menopause. Endocrinology & Metabol Clin North Am 26:279-294.
15. Seeman MV Psychopathology in women and men: focus on female hormones. Am J Psychiatry 154:1641-1647.
16. Smith JA Jr 1996 Management of hot flushes due to endocrine therapy for prostate carcinoma. Oncology 10:1319-1322.
17. Sugawara M, Toda MA, Shima S, Mukai T, Sakakura K, Kitamura T 1997 Premenstrual mood changes and maternal mental health in pregnancy and the postpartum period. J Clin Psychol 53:225-232.
18. Yonkers KA 1997 Anxiety symptoms and anxiety disorders: how are they related to premenstrual disorders?. J Clin Psychiatry 58:62-67.
19. Woodward S, Freedman RR 1994 The thermoregulatory effects of menopausal hot flushes on sleep. Sleep 17:497-501.
20. Fink G, Sumner BE, Rosie R, Grace O, Quinn JP 1996 Estrogen control of central neurotransmission: effect on mood, mental state, and memory. Cell Mol Neurobiol 16:325-344.
21. Rusak B, Zucker I. 1975 Biological rhythms and animal behavior. Annual Review of Psichology 26:137-171.
22. Moore RY. 1983 Organization and function of a central nervous system circadian oscillator: the suprachiasmatic hypothalamic nucleus. Fed Proc 42:2783-2789.
23. Moore RY. 1973 Retinohypothalamic projection in mammals: a comparative study. Brain Res 49:403-409.
24. Moore RY, Lenn NJ. 1972 A retinohypothalamic projection in the rat. J Comp Neurol 146:1-14.
25. Hendrickson AE, Wagoner W, Cowan WM. 1972 An autoradiographic and electron microscopic study of retinohypothalamic connections. Z Zellforsch 135:1-36.

26. Silver R, LeSauter J, Tresco PA, Lehman MN 1996 A diffusable coupling signal from the transplanted suprachiasmatic nucleus controlling circadian locomotor rhythms. Nature 382:810-813.

27. Watts AG, SwansonLW 1987 Efferet projections of the suprachiasmatic nucleus: II. Studies using retrograde transport of fluorescent dyes and simultaneous peptide immunohistochemistry in the rat. J Comp Neurol 258:230-252.

28. Watts AG, Swanson LW, Sanchez-Wattz G 1987 Efferent projections of the suprachiasmatic nucleus: I. Studies using anterograde transport of Phaseolus vulgaris leucoagglutinin in the rat. J Comp Neurol 258:204-229.

29. Ribak CE, Peters A 1975 An autoradiographic study of projections from the lateral geniculate body of the rat. Brain Res 92:341-368.

30. Swanson LW, Cowan WM, Jones EG 1974 An autoradiographic study of the efferent projections of the ventral lateral geniculate nucleus in the albino rat and cat. J Comp Neurol 156:143-164.

31. Samson WK, McCann SM 1979 Effects of suprachiasmatic nucleus lesions on hypothalamic LH-releasing hormone (GnRH) content and gonadotrophin secretion in the ovariectomized (OVX) female rat. Brain Research. Bulletin. 4:783-788.

32. Harris GW 1972 Humours and hormones. J. of Endocrinology, 53: ii-xxiii.

33. Ben-Jonathan N 1985 Dopamine: a prolactin-inhibiting hormone. Endocr Rev 6:564-589.

34. Antunes-Rodriques J and McCann SM 1967 Effect of suprachiasmatic nucleus lesions on the regulation of luteinizing hormone secretion in the female rat. Endocrinology 81:666-670.

35. Brown-Grant K and Raisman G 1977 Abnormalities in reproductive function associated with destruction of the suprachiasmatic nuclei in female rats. Proc R Soc London 198:279-296.

36. Kawakami M, Arita J, Yoshioka E 1980 Loss of oestrogen-induced daily surges of prolactin and gonadotrophins by suprachiasmatic nucleus lesions in ovariectomized rats. Endocrinology 106:1087-1092.

37. Pan JT, Gala RR 1985 Central nervous system regions involved in the estrogen-induced afternoon prolactin surge. I. Lesion studies. Endocrinology 117:382-387.

38. Brown-Grant K, Davidson JM, Greig F 1973 Induced ovulation in albino rats exposed to constant light. J Endocrinology 57:7-22.

39. Critchlow V 1963 The role of light in neuroendocrine system. In: Advances in Neuroendocrinology (Nalbanov AV, ed), pp: 377-402. Urbana: University of Illinois Press.

40. Nir I, Hirschmann N 1982 Effect of constant light and darkness on pituitary and serum gonadotropin and sex hormone levels of parturient rats. J Neural Transmission 55:157-168.

41. Vaticon MD, Fernandez-Galaz C, Esquifino A, Tejero A, Aguilar E 1980 Effects of constant light on prolactin secretion in adult female rats. Hormone Res 12:277-288.

42. Pieper DR, Gala RR 1979 The effect of light on the prolactin surges of pseudopregnant and ovariectomized rats. Biol Reprod 20:7727-732.

43. Sartin JL, Bruot BC, Orts RJ 1981 Changes in serum prolactin following blinding and constant light exposure. J Endocrinological Investigation 4:97-108.

44. Sterner MR, Cohen IR 1995 Steroid treatment fails to induce an afternoon luteinizing hormone or prolactin surge in rats exposed to short-term constant light at the time of ovariectomy. Neuroendocrinology 62:231-237.

45. Watts AG, Fink G 1981 Effects of short-term constant light on the proestrous luteinizing hormone surge and pituitary responsiveness in the female rat. Neuroendocrinology 33:176-180.

46. Watts AG, Fink G 1981 Constant light blocks diurnal but not pulsatile release of luteinizing hormone in the ovariectomized rat. J Endocrinol 89:141-146.

47. Kawano H, Daikoku S 1987 Functional topography of the rat hypothalamic dopamine neuron systems: Retrograde tracing and immunocytochemical study. J Comp Neurol 265:242-253.

48. Chan-Palay V, Zaborszky L, Köhler C, Goldstein M, Palay SL 1984 Distribution of tyrosine-hydroxylase immunoreactive neurons in the hypothalamus of rats. J Comp Neurol 227:467-494.

49. van den Pol A, Herbst R, Powel J 1984 Tyrosine hydroxylase immunoreactive neurons of the hypothalamus. A light and electron microscopic study. Neuroscience 13:1117-1156.

50. Honma KI and Hiroshige T 1978 Internal synchronization among several circadian rhythms in rats under constant light. American Journal of Physiology. 235:R244-249.

51. Morimoto Y, Oishi T, Arisue K, Ogawa Z, Tanaka F 1975 Circadian rhythm of plasma corticosteroid in adult female rats: chronological shifts in abnormal lighting regimens and connection with oestrus cycle. Acta Endocrinologica (Copemh) 80:527-541.

52. Hickey TL and Spear PD 1976 Retinogeniculate projections in hooded and albino rats: an autoradiographic study. Experimental Brain Research 24:523-529.

53. Mikkelsen JD 1990 A neuronal projection from the lateral geniculate nucleus to the lateral hypothalamus of the rat demonstrated with Phaseolus vulgaris leucoagglutinin tracing. Neuroscience Letters 116:58-63.

54. Mikkelsen JD 1990 Projections from the lateral geniculate nucleus to the hypothalamus of the Mongolian gerbil (Meriones unguiculatus): an anterograde tracing study. J Comp Neurol 299:493-508.

55. Moore RY, Moga MM, Weis R 1996 Intergeniculate leaflet (IGL) and ventral lateral geniculate (VLG) projections in the rat. 26th Annual Meeting of the Society for Neuroscience, Washington DC, Abstract # 65.8.

56. Albers HE, Moline ML, Moore-Ede MC 1984 Sex differences in circadian control of LH secretion. J Endocrinology 100:101-105.

57. Legan SJ, Karsch FJ 1975 A daily signal for the LH surge in the rat. Endocrinology 96:57-62.

58. Ma YJ, Kelly MJ, Ronnekleiv OK 1990 Pro-gonadotrophin-releasing hormone (pro-GnRH) and GnRH content in the preoptic area and the basal hypothalamus of anterior medial preoptic nucleus/ suprachiasmatic nucleus lesioned rats. Endocrinology 127:2654-2664.

59. Fink G,Rosie R,Thomson E 1991 Steroid actions on hypothalamic neurons with special reference to estrogen control of luteinizing hormone-releasing hormone biosynthesis and release volume transmission in the brain: Novel mechanisms for neuronal transmission. Fuxe K, Agnati LF (eds), Raven Press New York, 195-211.

60. Le Blond CB, Morris S, Karakiulakis G, Powell R, Thomas PJ 1982 Development of sexual dimorphism in the suprachiasmatic nucleus of the rat. J Endocrinol 95:137-145.

61. Swaab DF, Fliers E, Partiman TS 1984 The suprachiasmatic nucleus of the human brain in relation to sex, age and senile dementia. Brain Res 342:37-44.

62. Güldner FH 1983 Numbers of neurons and astroglial cells in the suprachiasmatic nucleus of male and female rats. Exp Brain Res 50:373-376.

63. Watson RE, Wiegand SJ, Clough RW, Sladek CD and Hoffman-Small GE 1984 The sexuallt dimorphic vasopressinergic fiber density in the medial preoptic nucleus originates in the suprachiasmatic nucleus. Soc for Neurosci Abst 10, Abstract # 129.9

64. Horvath TL, Cela V, van der Beek EM 1998 Gender specific apposition of vasoactive intestinal peptide-containing axons on gonadotrophin-releasing hormone neurons in the rat. Brain Research 795:277-281.

65. Södersten P, Hansen S, Srebro B 1981 Suprachiasmatic lesios disrupt the daily rhythmicity in the sexual bahaviour of normal male rats and of male rats treated neonatally with antioestrogen. J Endocrinol 88:125-130.

66. Gorski RA, Harlan RE, Jacobson CD, Shryne JE, Southam AM 1980 Evidence for the existence of a sexually dimorphic nucleus in the preoptic area of the rat. J Comp Neurol 193:529-539.

67. Gorski RA, Gordon JH, Shryne JE, Southam AM 1978 Evidence for a morphological sex difference within the medial preoptic area of the rat brain. Brain Res 148:333-346.

68. Döhler KD, Coquelin A, Davis F, Hines M, Shryne JE, Gorski RA 1982 Differentiation of the sexually dimorphic nucleus in the preoptic area of the rat brain is determined by the perinatal hormone environment. Neurosci Lett 33:295-298.

69. Döhler KD, Hines M, Coquelin A, Davis F, Shryne JE, Gorski RA 1982 Pre- and postnatal influence of diethylstilboestrol on differentiation of the sexually dimorphic nucleus int the preoptic area of the female rat brain. Neuroendocrinol Lett 4:361-365.

70. Gorski RA 1980 Sexual differentiation of the brain. In: Neuroendocrinology: The interrelationship of the body's two major integrative systems-in normal physiology and in clinical disease. (Krieger DT and Hughes JC eds), Sinauer Associates, Sunderland, pp:216-222.

71. Weisz J, Ward IL 1980 Plasma testosterone and progesterone titers of pregnant rats, their male and female fetuses, and neonatal offspring. Endocrinology 106:306-316.

72. Jacobson CD, Csernus VJ, Shryne JE, Gorski RA. 1981 The influence of gonadectomy, androgen exposure, or a gonadal graft in the neonatal rat on the volume of the sexually dimorphic nucleus of the preoptic area. J. Neurosci 1:1142-1147.

73. Naftolin F, Ryan KJ, Davis IJ, Reddy VV, Flores F, Petro Z, Kuhn M. 1975 The formation of estrogens by central neuroendocrine tissues. Recent Prog Horm Res 31: 295-319.

74. Reddy VVR, Naftolin F, Ryan KJ 1974 Convertion of androstenedione to estrone by neural tissues from fetal and neonatal rats. Endocrinology 94:117-121.

75. Roselli CE, Resko JA 1993 Aromatase activity in the brain: hormonal regulation and sex differences. J Steroid Bioch Mol Biol 44:499-508.

76. Bunt SM, Lund RD, Land PW 1983 Prenatal development of the optic projection in albino and hooded rats. Dev Brain Res 6: 149-168.

77. MacLusky NJ, Philip A, Hurlburt C, Naftolin F 1985 Estrogen formation in the developing rat brain: sex differences in aromatase activity during early post-natal life. Psychoneuroendocrinology 10:355-361.

78. Wuttke W, Döhler KD 1975 Changes with age in levels of serum gonadotrophins, prolactin, and gonadal steroids in prepubertal male and female rats. Endocrinology 97:898-907.

79. Forest MG 1979 Plasma androgens (testosterone and 4-androstendione) and 17-hydroxyprogesterone in the neonatal prepubertal and peripubertal periods in the human and the rat: differences between species. J Steroid Biochem 11:543-548.

80. Miyachi Y, Nieschlag E, Lipsett MB 1973 The secretion of gonadotrophins and testosterone by neonatal male rat. Endocrinology 92:1-5.

81. Horvath TL, Roa-Pena L, Wikler K, Naftolin F 1994 Estrogen synthetase (aromatase) immunoreactivity in the developing rat visual system. 24th Ann Meeting of Soc for Neurosci, Miami, FL, Abstact 364.7, p: 869.

82. Horvath TL, Wikler KC 1998 Aromatase in developing sensory systems of the rat. J Neuroendocrinology (in press).

83. Lenn NJ, Beebe B, Moore RY 1977 Postnatal development of the suprachiasmatic hypothalamic nucleus of the rat. Cell Tiss Res.178:463-475.

84. Paxinos G, Watson C 1986 The rat brain in stereotaxic coordinates. Academic Press, Orlando.

85. Merchenthaler I 1991 Neurons with access to the general circulation in the central nervous system of the rat: a retrograde tracing study with fluoro-gold. Neuroscience 44:655-662.

86. Merchenthaler I 1991 The hypophysiotropic galanin system of the rat brain. Neuroscience 44:643-654.

87. Shughrue PJ, Lane MV, Merchenthaler I 1997 Comparative distribution of estrogen receptor-alpha and –beta mRNA in the rat central nervous system. J Comp Neurol 388:507-525.

88. Shughure PJ, Lane, Merchenthaler I 1997 Regulation of progesterone receptor messenger ribonucleic acid in the rat medial preoptic nucleus by estrogenic and antiestrogenic compounds: an in situ hybridization study. Endocrinology 138:5476-5484.

89. Sanghera, MK, Simpson ER, McPhaul MJ, Kozlowski G, Coney AJ, Lephard ED 1991 Immunocytochemical distribution of aromatase cytochrome P450 in the rat brain using peptide-generated polyclonal antibodies. Endocrinology. 129:2834-2844.

90. Horvath, TL, Roa-Pena L, Jakab RL, Simpson E, Naftolin F 1997 Aromatase in axonal processes of early postnatal hypothalamic and limbic areas including the cingulate cortex. J. Steroid Biochem. Molec. Biol. 61:349-357.

91. Balthazart, J, Foidart A, Surlemont C, Harada N 1991 Distribution of aromatase-immunoreactive cells in the mouse forebrain. Cell. Tissue. Res. 263:71-79.

92. Jakab, RL, Horvath TL, Leranth C, Harada N, Naftolin F 1993 Aromatase immunoreactivity in the rat brain: gonadectomy-sensitive hypothalamic neurons and unresponsive "limbic ring" of the lateral septum-bed nucleus-amygdala complex. J Steroid Biochem. Mol. Biol. 44:481-498.

93. Naftolin, F, Horvath TL, Jakab RL, Leranth C, Harada N, Balthazart J 1996 Aromatase immunoreactivity in axon terminals of the vertebrate brain; An immunocytochemical study on quail, rat, monkey and human tissues. Neuroendocrinology. 63:149-155.

94. Horvath TL, Kalra SP, Naftolin F, Leranth C 1995 Morphological evidence for a galanin - opiate interaction in the rat mediobasal hypothalamus. J. Neuroendocrinology 7:579-588.

95. van der Beek, E.M., Wiegant V.M., van der Donk H.A., van den Hurk R. and Buijs R.M 1993 Lesions of the suprachiasmatic nucleus indicate the presence of a direct vasoactive intestinal polypeptide-containing projection to gonadotrophin-releasing hormone neurons in the female rat, J. Neuroendocrinol., 5:137-144.

96. de la Iglesia HO, Blaustein JD, Bittman EL 1995 The suprachiasmatic area of the female hamster projects to neurons containing estrogen receptors and GnRH. Neuroreport. 6(13):1715-1722.

97. van den Pol A, Herbst R, Powel J 1984 Tyrosine hydroxylase immunoreactive neurons of the hypothalamus. A light and electron microscopic study. Neuroscience 13:1117-1156.

98. Horvath TL, Naftolin F, and Leranth C 1992 β-endorphin innervation of dopamine neurons in the rat hypothalamus, a light and electron microscopic double immunostaining study. Endocrinology 131:1547-1555.

99. Horvath TL, Naftolin F, and Leranth C 1992 GABAergic and catecholaminergic innervation of mediobasal hypothalamic β-endorphin cells projecting to the medial preoptic area. Neuroscience 51:391-399.

100. Jonsson G, Fuxe K, Hokfelt T 1971 On the catecholamine innervation of the hypothalamus, with special reference to the median eminence. Brain Res 40:271-281.

101. Horvath TL 1997 Suprachiasmatic efferents avoid phenestrated capillaries but innervate neuroendocrine cells including those producing dopamine. Endocrinology 138:1312-1320.

102. Morin LP, Blanchard J 1993 Organization of the hamster paraventricular hypothalamic nucleus. Journal of Coparative Neurology 332:341-357.

103. Takatsuji K, Miguel-Hialgo J-V, Tohyama M 1991 Retinal fibers make synaptic contact with neuropeptide Y and enkephalin immunoreactive neurons in the intergeniculate leaflet of the rat. Neuroscience Lett 125:73-76.

104. Shinoda, K, Nagano M, Osawa Y 1994 Neuronal aromatase expression in preoptic, strial and amygdaloid regions during late prenatal and early postnatal development in the rat. J. Comp. Neurol. 343:113-129.

105. Wray, S., Hoffman G 1986 A developmental study of the quantitative distribution of LHRH neurons within the central nervous system of postnatal male and female rats. J .Comp. Neurol. 252:522-531.

106. van der Beek, E.M., van Oudheusden H.J.C., Buijs R.M., van der Donk H.A. and Wiegant V.M 1993 Preferential induction of c-fos immunoreactivity in vasoactive intestinal polypeptide-innervated gonadotropin-releasing hormone neurons during a steroid-induced luteinizing hormone surge in the female rat. Endocrinol., 134:2636-2644.

107. Chen, W.P., Witkin J.W.and Silverman A.J 1990 Sexual dimorphism in the synaptic input to gonadotrophin releasing hormone neurons. Endocrinol. 126:695-702.

108. Brian J. Oldfield, Michael J. McKinley 1995 Circumventricular Organs. In: The rat nervous system (Paxinos G ed), Academic Press, New York, pp:391-404.

109. Elde R, Hokfelt T 1979 Localization of hypophysiotropic peptides and other biologically active peptides within the brain. Annu Rev Physiol 41:587-602.

110. Goldsmith PC, Ganong WF 1975 Ultrastructural localization of luteinizing hormone-releasing hormone in the median eminence of the rat. Brain Res 97:181-193.

111. Kordon C, Kerdelhue B, Pattou E, Jutisz M, Sawyer CH 1974 Immunocytochemical localization of LHRH in axons and nerve terminals of the rat median eminence. Proc Soc Exp Biol Med 147:122-127.

112. Watkins WB, Schwabedal P, Bock R 1974 Immunohistochemical demonstration of a CRF-associated neurophysin in the external zone of the rat median eminence. Cell Tissue Res 152:411-421.

113. Takahara J, Arimura A, Schally AV 1975 Assessment of GH releasing hormone activity in sephadex-separated fractions of porcine hypothalamic extracts by hypophyseal portal vessel infusion in the rat. Acta Endocrinologica 78:428-434.

114. Hokfelt T, Fuxe K, Johansson O, Jeffcoate S, White N 1975 Distribution of tyrotropin-releasing hormone (TRH) in the central nervous system as revealed with immunohistochemistry. Eur J Pharmacol 34:389-392.

115. Hokfelt T, Efendic S, Hellerstrom C, Johansson O, Luft R, Arimura A 1975 Cellular localization of somatostatin in endocrine-like cells and neurons of the rat with special references to the A1-cells of the pancreatic islets and too the hypothalamus. Acta Endocrin Suppl (Copenh) 200:5-41.

116. Hokfelt T 1967 The possible ultrastructural identification of tubero-infundibular dopamine containing nerve endings in the median eminence of the rat. Brain Res 5:121-123.

117. Hamon M, Javoy F, Kardon C, Glowinski J 1970 Synthesis and release of serotonin in the median eminence of the rat. Life Sci 9:167-173.

118. Ajika K, Ochi J 1978 Serotoninergic projections to the suprachiasmatic nucleus and median eminence of the rat: identification by fluorescence and electron microscope. J Anat 127:563-576.

119. Fiok J, Acs Z, Makara GB, Erdo SL 1984 Site of gamma-aminobutyric acid (GABA)-mediated inhibition of growth hormone secretion in the rat. Neuroendocrinology 39:510-516.

120. Tappaz ML, Wassef M, Oertel WH, Paut L, Pujol JF 1983 Light- and electron-microscopic immunocytochemistry of glutamic acid decarboxylase (GAD) in the basal hypothalamus:

morphological evidence for neuroendocrine gamma-aminobutyrate (GABA). Neuroscience 9:271-287.

121. van der Beek EM, Horvath TL, Wiegant VM and Buijs RM 1996 Evidence for a direct neuronal pathway from the suprachiasmatic nucleus to the gonadotropin-releasing hormone system: Combined tracing and light- and electron-microscopical immunocytochemical studies. J comp Neurol (in press).
122. Bjorklund A, Lindwall O, Nobin A 1975 Evidence of an incerto-hypothalamic dopamine neuron system in the rat. Brain Res 89:29-42.
123. Swanson L, Sawchenko P, Berod A, Hartman B, Helle K, Vanorden D 1981 An immunohistochemical study of the organization of catecholaminergic cells and terminal fields in the paraventricular and supraoptic nuclei of the hypothalamus. J Comp Neurol 196:271-285.
124. Horvath TL, Naftolin F, and Leranth C 1993 Luteinizing hormone-releasing hormone and gamma aminobutiric acid neurons in the medial preoptic area are synaptic targets of dopamine axons originating in anterior periventricular areas. J Neuroendocrinology 5:71-79.34.
125. Döhler KD, Wuttke W 1976 Circadian fluctuations of serum hormone levels in prepubertal male and female rats. Acta Endocrinologica 83:269-279.
126. Legan SJ, Karsch FJ 1975 A daily signal for the LH surge in the rat. Endocrinology 96:57-62.
127. Turek FW, Van Cauter E 1988 Rhythms in reproduction. In: The physiology of reproduction. (Knobil E and Neill J eds.), Ravenn Press, New York, pp:1789-1831.
128. Wiegand SJ, Terasawa E 1982 Discrete lesions reveal functional heterogeneity of suprachiasmatic structures in regulation of gonadotrophin secretion in the female rat. Neuroendocrinology 34: 395-404.
129. Ben-Jonathan N, Oliver C, Weiner HJ, Mical RS, Porter JC 1977 Dopamine in hypophysial portal plasma of the rat during the estrus cycle and throughout pregnancy. Endocrinology 100:452-458.
130. Smith MS, Freeman ME, Neill JD 1976 The control of progesterone secretion during the estrus cycle and early pseudopregnancy in the rat: prolactin, gonadotropin and steroid levels associated with rescue of the corpus luteum of pseudopregnancy. Endocrinology 96:219-226.
131. Neill JD, Freeman ME, Tilson SA 1971 Control of the proestrus surge of prolactin and luteinizing hormone secretion by estrogen in the rat. Endocrinology 89:1448-1453.

132. Mai LM, Shieh KR, Pan JT 1994 Circadian changes of serum prolactin levels and tuberoinfundibular dopaminergic neuron activities in ovariectomized rats treated with or without estrogen: The role of the suprachiasmatic nucleus. Neuroendocrinology 60:520-526.

133. Card JP, Brecha N, Karten HJ, Moore RY 1981 Immunocytochemical localization of vasoactive intestinal polypeptide-containing cells and processes in the suprachiasmatic nucleus of the rat: light and electron microscopic analysis. J Neurosci 1:1289-1303.

134. Buijs RM, Hou Y-X, Shinn S, Renaud LP 1993 Ultrastructural evidence for intra- and extra-nuclear projections of GABA-ergic neurons of the suprachiasmatic nucleus. J Comp Neurol 340:381-391.

135. Watson RE Jr, Langub MC Jr, Engle MG, Maley BE 1995 Estrogen-receptive neurons in the anteroventral periventricular nucleus are synaptic targets of the suprachiasmatic nucleus and peri-suprachiasmatic region. Brain Res 689:254-264.

136. Swanson LW, Cowan WM, Jones EG 1974 An autoradiographic study of the efferent projections of the ventral lateral geniculate nucleus in the albino rat and cat. J Comp Neurol 156:143-164.

137. Ribak CE and Seress L 1983 Five types of basket cells in the hippocampal dentate gyrus: A combined Golgi and electron microscopic study. J Comp Neurol 12:577-597.

138. Mantyh PW and Kemp JA 1983 The distribution of putative neurotransmitters in the lateral geniculate nucleus of the rat. Brain Research 288:344-348.

139. Takatsuji K and Tohyama M 1989 The organization of the rat lateral geniculate body by immunocytochemical analysis of neuroactive substances. Brain Research 480:198-209.

140. Moore RY, Speh JC 1993 GABA is the principal neurotransmitter of the circadian system. Neuroscience Letters 150:112-116.

141. Moore RY, Card JP 1994 Intergeniculate leaflet: an anatomically and functionally distinct subdivision of the lateral geniculate comples. Journal of Comparative Neurology 344:403-430.

142. Johnson RF, Morin LP, Moore RY 1988 Retinohypothalamic projections in the hamster and rat demonstrated using cholera toxin. Brain Research 462:301-312.

143. Levine JD, Zhao X-S, Miselis RR 1994 Direct and indirect retinohypothalamic projections to the supraoptic nucleus in the female albino rat. J Comp Neurol 341:214-224.

144. Mikkelsen JD 1992 Visualization of efferent retinal projections by immunocytochemical identification of cholera toxin subunit B. Brain Res Bull 28:619-623.

145. Pickard GE, Silverman JA 1981 Direct retinal projections to the hypothalamus piriform cortex, and accessory optic nuclei in the golden hamsters as demonstrated by a sensitive anterograde horseradish peroxidase technique. J Comp Neurol 196:155-172.

146. Riley JN, Card JP, Moore RY 1981 A retinal projection to the lateral hypothalamus in the rat. Cell Tissue Res 214:257-269.

147. Moore RY, Moga MM, Weis R 1996 Intergeniculate leaflet (IGL) and ventral lateral geniculate (VLG) projections in the rat. 26th Annual Meeting of the Society for Neuroscience, Washington DC, Abstract # 65.8.

148. Morin LP, Cummings LA 1982 Splitting of wheelrunning rhythms by castrated or steroid treated male and female hamsters. Physiol Behav 29:665-675.

149. Pickard GE, Turek FW 1982 Splitting of the circadian rhythm of activity is abolished by unilateral lesions of the suprachiasmatic nuclei. Science 215:1119-1121.

150. Pittendrigh CS, Daan S 1976 A functional analysis of the circadian pacemakers in nocturnal rodents. V. Pacemakers structure: A clock for all season. J Comp Physiol 106:333-355.

151. Swann J, Turek FW 1982 Cycle of lordosis behavior in female hamsters whose circadian activity rhythm has split into two components. American J Physiology 243:112-118.

152. Swann JM, Turek FW 1985 Multiple circadian oscillators regulate the timing of behavioral and endocrine rhythms in female golden hamsters. Science 228:898-900.

153. Edelstein K, Amir S 1996 Constant light induces persistent Fos expression in rat intergeniculate leaflet. Brain Res 731:221-225.

154. Park HT, Beak SY, Kim BS, Kim JB, Kim JJ 1993 Profile of Fos-like immunoreactivity induction by light stimuli in the intergeniculate leaflet is different from that of the suprachiasmatic nucleus. Brain Res 610:334-339.

155. Naftolin, F, Ryan KJ, Petro Z 1971 Aromatization of androstendion by the diencephalon. J. Clin. Endocrinol. Metabol. 33:368-370.

156. Arnold, AP, Gorski RA 1984 Gonadal steroid induction of structural sex differences in the central nervous system. Ann. Rev. Neurosci. 7:48-69.

157. McEwen, BS 1980 Binding and metabolism of sex steroids by the hypothalamic-pituitary unit: physiological implications. Ann. Rev. Physiol. 42:97-110.

158. Roselli, CE, Resko JA 1989 Testosterone regulates aromatase activity in discrete brain areas of the male rhesus macaques. Biol. Reprod. 40:929-934.

159. Callard, GV 1984 Aromatization in brain and pituitary: an evolutionary perspective. In F. Celotti, F. Naftolin and L. Martini (Eds.), Metabolism of hormonal steroids in the neuroendocrine structures, Raven Press, New York, pp. 79-102.

160. Shinoda, K, Yagi H, Fujita H, Osawa Y, Shiotani Y 1989 Screening of aromatase-containing neurons in the rat forebrain: An immunohistochemical study with antibody against the human placental antigen X-P_2 (hPAX-P_2). J. Comp. Neurol. 290:502-515.

161. Shinoda, K, Yagi H, Osawa Y, Shiotani Y 1990 Involvement of specific placental antigen X-P_2 in rat olfaction: an immunohistochemical study of the olfactory bulb. J. Comp. Neurol. 294:340-344.

162. Shinoda, K, Mori S, Ohtsuki T, Osawa Y 1992 An aromatase-associated cytoplasmic inclusion, the "stigmoid body" in the rat brain: I Distribution in the forebrain. J. Comp. Neurol. 322:360-376.

163. Shinoda, K, Nagano M, Osawa Y 1993 An aromatase-associated cytoplasmic inclusion, the "stigmoid body" in the rat brain: II Ultrastructure (with a review of its history and nomenvlature). J. Comp. Neurol. 329:1-19.

164. Lauber, ME, Lichtensteiger W 1994 Pre- and postnatal ontogeny of aromatase cytochrome P450 messenger ribonucleic acis expression in the male rat brain studied by in situ hybridization. Endocrinology . 135:1661-1668.

165. Wagner, CK, Morrell JI. 1996 Distribution and steroid hormone regulation of aromatase mRNA expression in the forebrain of adult male and female rats: a cellular-level analysis using in situ hybridization. J. Comp. Neurol. 370:71-84.

166. Schlinger, BA, Callard GV 1989 Localization of aromatase in synaptosomal and microsomal subfractions of quail (Coturnix coturnic japonica) brain. Neuroendocrinology. 49:431-441.

167. MacLusky, NJ, Walters MJ, Clark AS, Toran-Allerand CD 1994 Aromatase in the cerebral cortex, hippocampus, and mid-brain: ontogeny and developmental implications. Molecular and Cellular Neurosciences. 5:691-698.

168. Weisz, J, Ward IL 1980 Plasma testosterone and progesterone titers of pregnant rats, their male and female fetuses, and neonatal offspring. Endocrinology. 106:306-316.

169. Forest, MG 1979 Plasma androgens (testosterone and 4-androstenedione) and 17-hydroxyprogesterone in the neonatal prepuberal and peripubertal periods in the human and the rat: differences between species. J. Steroid. Biochem. 11:543-548.

170. Davis, EC, Popper P, Gorski RA 1996 The role of apoptosis in sexual differentiation of tyhe rat sexually dimoprhic nucleus of the preoptic area. Brain Res. 734:10-18.

171. Toran-Allerand, CD 1976 Sex steroids and the development of the newborn mouse hypothalamus and preoptic area in vitro: implication for sexual differentiation. Brain Res. 106:407-412.

172. Perez, J, Naftolin F, Garcia-Segura LM 1990 Sexual differentiation of synaptic connectivity and neural plasma membrane in the arcuate nucleus of the rat hypothalamus. Brain Res. 527:116-120.

173. Segovia, S, Guillamon A 1993 Sexual dimorphism in the vomeronasal pathway and sex differences in reproductive behaviors. Brain Reserach Reviews 18:51-74.

174. Juraska, JM. 1991 Sex differences in "cognitive" regions of the rat brain. Psychoneuroendocrinology. 16:105-119.

175. Callard, GV, Drygas M, Gelinas D 1993 Molecular and cellular physiology of aromatase in the brain and retina. J. Steriod Biochem. Molec. Biol. 44:541-547.

176. Lephart ED 1996 A review of brain aromatase cytochrome P450. Brain Res. Rev. 22:1-26.

177. Simerly, RB, Chang C, Muramatsu M and Swanson LW 1990 Distribution of androgen and estrogen receptor-containing cells in the rat brain: an in situ hybridization study. J. Comp. Neurol. 294:76-95.

178. Simonian, SX, Herbison AE 1997 Differential expression of estrogen receptor and neuropeptide Y by brainstem A1 and A2 noradrenaline neurons. Neuroscience. 76:517-529.

179. Gorski, R.A 1973 Perinatal effects of sex steroids on brain development and function. Prog Brain Res 39:149-162.

180. Pfeiffer, C.A 1936 Sexual differences of the hypophyses and their determination by gonads. Am. J. Anat., 58:195-225.

181. Loke, D.M.F., Ratnam S.S. and Goh H.H 1992 Luteinizing hormone surge in adult female rats after androgen priming. J. Neuroendocrinol., 4:211-215.

182. Riskind, P.N., Allen J.M., Gabriel S.M., Koenig J.I. and Audet-Arnold J 1989 Sex difference in vasoactive intestinal peptide (VIP) concentrations in the anterior pituitary and hypothalamus of rats. Neurosci. Lett., 105:215-220.

183. Gozes, I., and Brenneman D.E 1989 VIP: molecular biology and neurobiological function. Mol.. Neurobiol.,. 3:201-236.

184. Lakhdar-Ghazal, N., Kalsbeek A. and Pevet P 1992 Sexual differences and seasonal variations in vasoactive intestinal peptide immunoreactivity in the suprachiasmatic nucleus of jerboa (Jaculus orientalis). Neurosci. Lett. 144:29-33.

185. Harney, J.P., Scarbrough K., Rosewell K.L. and Wise P.M 1996 In vivo antisense antagonism of vasoactive intestinal peptide in the suprachiasmatic nucleus causes aging-like changes in the estradiol-induced luteinizing hormone and prolactin surges. Endocrinol., 137:3696-3701.

186. Kimura, F., Mitsugi N., Arita J., Akema T. and Yoshida K 1987 Effects of preoptic injections of gastrin, cholecystokinin, secretin, vasoactive intestinal polypeptide and PHI on the secretion of luteinizing hormone and prolactin in ovariectomized estrogen-primed rats. Brain Res., 410:315-322.

187. Weick, R.F. and Stobie K.M 1992 Vasoactive intestinal peptide inhibits the steroid-induced LH surge in the ovariectomized rat. J. Endocrinol., 133:433-437.

188. Gray, G.D., Sodersten P., Tallentire D. and Davidson J.M 1978 Effects of lesions in various structures of the suprachiasmatic-preoptic region on LH regulation and sexual behaviour in female rats, Neuroendocrinol., 25:174-191.

ANATÓMIAI KAPCSOLAT A BIOLÓGIAI ÓRA ÉS A SZAPORODÁS AGYI SZABÁLYOZÁSÁÉRT FELELÖS HIPOTHALAMIKUS SEJTCSOPORTOK KÖZÖTT

(MAGYAR NYELVŰ ÖSSZEFOGLALÓ)

Bevezetés, célok

A központi idegrendszer normális működéséhez elengedhetetlen bizonyos alapvető biológiai mechanizmusok összehangolt szabályozása. Ezt, a legtöbb esettben ritmikus együtműködését a különféle autonóm és endokrin folyamatoknak, a hipothalamikus nukleusz szuprakiazmatiszban elhelyezkedő biologiai óra végzi.

Míg a biológiai óráról és annak fényviszonyokat közvetítő szerepéről nagy mennyiségű kisérletes adat áll rendelkezésünkre, kevésbe ismert az, hogy a hipothalamikus nukleusz szuprakiazmatisz által létrehozott jelek milyen módon jutnak el a különféle endokrin és autonóm szabályozásokért felelős agyi magcsoportokba.

A biológiai óra működésének további megismerése érdekében, ezen disszertáció kisérleteiben arra kerestem választ, hogy milyen pályákon juthat el információ a biológiai órából azon hipothalamikus sejtekhez amelyek közvetlenül befolyásolják az elülső hipofizisben termelődő tejlelválasztást serkentő-(prolaktin) illetve sárgatestfejlesztő (luteinizing hormon; LH) hormonok termelését. Mivel ezen hormonok ritmikus termelése és kiválasztása nemtől függő folyamat, azt is feltételeztem, hogy egy, a korai egyedfejlődés során működő agyi mechanizmus a biológiai órára is hatással van.

A következő kérdések megválaszolását tűztem ki célul:

1) A szuprakiazmatikus magcsoport direkt kapcsolatban áll-e neuroendokrin sejtekkel amelyek LH serkentő hormont (LHRH) vagy dopamint termelnek. Ez utóbbi a prolaktin termelésének egyik fontos hipothalamikus szabályozója.
2) A nukleusz genikulátisz laterálisz, amely közvetlen kapcsolatban áll a biológiai órával, beidegez-e neuroendokrin sejteket a hipothalamuszban, ezáltal biztosítva fény információ eljutását a hipofizisbe a nukleusz szuprakiazmatisz megkerülésével?
3) Lehetséges-e, hogy hormon jelek a perifériáról befolyásolják a neuroendockrin sejteket a nukleusz genikulátisz laterăliszon keresztül?

4) Befolyásolhatja-e a biológiai óra fejlődését egy, a nemi elkülönülésért felelős mechanizmus?
5) Van-e nemi különbség az LHRH sejtek neurális inputjában amely a biológiai órából ered ?

Anyag és módszerek

Az első két kérdés magválaszolását anterográd, retrográd pályajelölés, akut axondegeneráció és fény valamint elektron mikroszkópos immunhisztokémiai eljárások kombinációjával végeztem el

Annak vizsgálatát, hogy ösztrogén vagy progeszteron direkt befolyásolja-e sejtek működését a nukleusz genikulátisz lateráliszban, mRNS *in situ* hybridizációt alkalmaztunk ösztrogén receptor β és progeszteron receptorok kimutatására.

Annak megválaszolására, hogy a korai egyedfejlődés során a biológiai óra hatása alatt van-e a nemi elkülönülésért felelős aromatáz enzimnek, immunohisztokémiai és biokémiai módszereket használtunk.

Azt a feltevést, hogy nemi különbség létezik a biológiai óra és az LHRH sejtek kapcsolatában, kavantitativ immunhisztokémiai eljárással elenőriztük.

Eredmények

1) Kisérleteink bizonyitották, hogy szinaptikus kapcsolat áll fenn a biológiai óra és neuroendokrin sejtek között. Ezen sejtek egy csoportja amellett, hogy közvetlen kapcsolatban állnak a portális kapillárisokkal, LHRH-t vagy dopamint is tartalmaznak.
2) Bizonyítást nyert, hogy fény jelek eljuthatnak a hipotalamusz neuroendokrin sejtjeihez a nukleusz szuprakiazmatisz megkerülésével, a talamikus nukleusz genikulátisz lateráliszon keresztül.
3) Kimuttatuk, hogy a nukleusz genikulátisz laterálisz ventrális és közbülső magcsopotjaiban sejtek termelnek mRNS-t amely az ösztrogén receptor β és progeszteron receptor génjeinek átírásáért felelősek. Ezáltal, figyelembe véve az előző kísérlet eredményeit, gyanítható, hogy az ovárium visszacsatolása a hipotalamuszra a talamuszon keresztül is történhet.

4) Bizonyítékot szolgáltattunk arra, hogy a korai egyedfejlődés folyamán, ami magában foglalja a késő prenatális és kora posztnatális időszakot a patkányban, az aromatáz enzim, amely felelős a nemi jellegek kialakításáért, jelen van mind a nukleusz szuprakiazmatiszban mint pedig a nukleusz genikulátisz laterálisban. Ez az eredmény arra enged következtetni, hogy bizonyos nemi különbségek léteznek a biológiai óra anatómiájában és működésében.
5) Kimutattuk, hogy a patkányban az LHRH sejtek beidegzése vazoaktiv interstitialis polipeptid (VIP) axonok által, amelyről előzőleg bizonyítást nyert, hogy a biológiai órából ered, masszívabb nőstény állatokban mint hímekben. Ez az eredmény tovább erősíti az a feltevést, hogy a szaporodás központi szabályozásáért felelős folyamatok nemi jellege részben a biológiai óra nemi sajátosságainak függvénye.

Összefoglalás

Ezen disszertáció eredményei anatómiai bizonyítékot szolgáltattak arra, hogy milyen úton juthat el információ a biológiai órából és a környezetből a neuroendokrin hipotalamuszba.
Azt is megállapítottuk, hogy a már ismert nemi elkülönülésért felelős fejlődési mechanizmus nem csak a hipotalamuszban és más limbikus régiókban fejtheti ki hatását, de eddig nem gyanított, érzekelésért felelős központi idegrendszeri területeken is. Mivel ezen területekhez tartozik a biológiai óra és a nukleusz genikulátisz laterálisz is, azt a következtetést vontuk le, hogy az elülső hipofízis nemtől függő szabályozása részben a biológiai óra sajátosságainak köszönhető.

Mivel a biológiai óra szerepet játszik a legtöbb autonóm es endokrin működés szabályozásában, gyanítható, hogy a központi idegrendszer egyéb ritmikus működései is nemtől és hormonoktól függő folyamat.